Spacecraft Angular Velocity Trajectory Planning for SGCMG Singularity Avoidance

Zhili Hou[1]

Tsinghua University, Shenzhen 518055, People's Republic of China

Yunhai Geng[2], Baolin Wu[3]

Harbin Institute of Technology, Harbin 150001, People's Republic of China

Simeng Huang[4]

Politecnico di Milano, Milano, 20156, Italy

A trajectory planning method for angular velocity of spacecraft is developed to avoid the impassable singular states for singular gimbal control moment gyroscope (SGCMG) systems in this paper. A new set of attitude parameters, named σ-parameters, is first developed. Based on the properties of σ-parameters, two approximate decoupled rotations are presented. To achieve a rapid attitude maneuver, both of the decoupled motions are designed as simple bang-off-bang type maneuvers. Then, a type of SGCMG singularity-free angular velocity trajectory on the conic surface is developed. Thereafter, an attitude controller based on σ-parameters is developed to track the reference trajectory. To avoid the impassable singular state, suitable axes of the approximate decoupled two rotations are chosen to achieve the fastest maneuver under the condition that the minimum distance from the angular momentum trajectory to the impassable surface is greater than a safety distance. Finally, simulations are performed to verify the effectiveness of the proposed SGCMG singularity avoidance method.

---

[1] Post-doctoral, Graduate School at Shenzhen; hzl1334123@163.com.
[2] Professor, Research Center of Satellite Technology; gengyh@hit.edu.cn.
[3] Associate Professor, Research Center of Satellite Technology; wubaolin@hit.edu.cn. Corresponding author.
[4] Ph.D. Student, Department of Aerospace Science and Technology; huangsm_hit@163.com.

I. Introduction

SGCMG is a type of commonly used actuator for spacecraft rapid maneuver due to its comparative mechanical simplicity and torque amplification capability. However, the inherent singularity of SGCMG systems renders their applications difficult. At a singular state, the produced torque cannot cover a three dimensional space. The internal singular states are classified as the passable and impassable singular state. The passable singular states can be easily avoided by adding a null motion to the pseudo-inverse solution [1, 2]. Therefore, attention is mainly paid to avoiding the impassable singular states, and many steering laws have been developed.

Magulies and Aubrun [3] developed the fundamental theories of the SGCMGs from the geometrical point of view. Kurokawa [4, 5] analyzed the corresponding solution in gimbal angle space for a certain angular momentum trajectory, and pointed out that no impassable singular state will be encountered for suitable initial gimbal angles. Vadali [6] then presented a method for choosing the initial gimbal angles to ensure that all of the impassable singular states were avoidable for a certain angular momentum trajectory. In addition to initial gimbal angles, another significant factor for singularity avoidance is the gimbal angle trajectory. To generate a suitable gimbal angle trajectory, a direct singularity avoidance method was developed in [7]. This method can avoid most of the singular states, but it is computation-intensive.

An impassable singular state is sure to be encountered for some inappropriate sets of initial gimbal angles. Then, the torque error must be induced to escape from the corresponding impassable singular surface. Nakamura and Hanafusa [8] presented a singular robust (SR) steering law, and this method was improved using an SVD method in [9–11]. Wie [12–14] summarized the theories of singularity robust steering laws and utilized a non-diagonal weighting matrix to effectively generate deterministic dither signals when gimbal angles are near the singular states. Fitz-Coy [15] presented a hybrid steering law ensuring the torque error and the null motion are small when the passable and impassable singular states are nearly approached, respectively. Takada [16] presented a singularity-avoidance steering law by adding a additional torque when angular momentum approaches the

impassable singular surface. Kurokawa [17, 18] developed a non-singularity and no torque error steering law for the pyramid configuration from another perspective. A linear constraint is added on the gimbal angles to re-constrain the angular momentum space, which guarantees no singular state in the re-constrained angular momentum space. Kanzawa [19] proposed a steering law ensuring the gimbal angles coverage to a set of target gimbal angles at the end of an attitude maneuver.

The impassable singular states will not be encountered if the reference angular momentum trajectory does not intersect with the impassable singular surface, which provides another hint for singular states avoidance. The idea is to design a suitable reference angular momentum trajectory for a fixed terminal attitude. Various angular trajectories were developed for various purposes, such as a time-optimal maneuvers [20, 21], and residual vibration suppression [22–24]. However, to the best of our knowledge, the problem of angular momentum trajectory planning to avoid impassable singular states of SGCMGs has not been addressed in the literature. The main reason is that it is challenging to describe the constraint that the reference angular trajectory should not intersect with the impassable singular surface.

This paper aims to develop a SGCMG singularity avoidance method by planning the angular momentum trajectory instead of planning the gimbal angle trajectory. Firstl, a new set of attitude parameters is developed. Based on the properties of this new set, an eigen-axis rotation is then decomposed as two approximate decoupled rotations with two perpendicular axes. Thereafter, a new type of angular velocity reference trajectory is developed by designing these two rotations respectively. Then, an attitude tracking controller with the proposed new set of attitude parameters is proposed to track the reference angular trajectory. Subsequently, the parameters of these two rotations are designed to avoid the impassable singular state by minimizing the maneuver time under the condition that the shortest distance from the angular momentum to the impassable surface is greater than a safety distance. Simulations results shows the effectiveness of the proposed SGCMG singularity avoidance method.

The main parts of this paper are organized as follows. Section II derives a new set of attitude parameters, and its kinematics. Section III develops a new type of reference angular velocity trajectory based on the properties of this new set of attitude parameters. Section IV proposes an attitude

controller using this new set of attitude parameters. Section IV presents a method for choosing suitable parameters of this new type of reference angular velocity trajectory to avoid the impassable singular states. Section V shows the simulation results.

II. Development of a New Set of Attitude Parameters

This section first develops a new set of attitude parameters, which are fundamental for the development of the new type angular velocity trajectory, presented in the next section, and then derives the kinematics of this set of attitude parameters. Finally, an attitude rotation is decoupled as two nearly independent rotations based on the properties of this new set of attitude parameters.

A. Definition of the New Set of Attitude Parameters

Before the development of the new attitude parameters, some coordinate frames are first defined as: Let $\mathcal{B}$ be a body fixed frame defined as follows. The origin is located at the center of mass of the spacecraft, and $\{\boldsymbol{x}_b, \boldsymbol{y}_b, \boldsymbol{z}_b\}$ are mutually orthogonal unit vectors fixed in the spacecraft body. Let $\mathcal{I}$ be an inertially fixed reference frame. Its origin is located at the center of mass of the Earth, and $\{\boldsymbol{x}_i, \boldsymbol{y}_i, \boldsymbol{z}_i\}$ are mutually orthogonal unit vectors fixed in inertial space. Let $\mathcal{T}$ be a target reference frame. Its origin is located at the center of mass of the spacecraft, and $\{\boldsymbol{x}_t, \boldsymbol{y}_t, \boldsymbol{z}_t\}$ are mutually orthogonal unit vectors fixed in inertial space, which represent the target direction of $\{\boldsymbol{x}_b, \boldsymbol{y}_b, \boldsymbol{z}_b\}$.

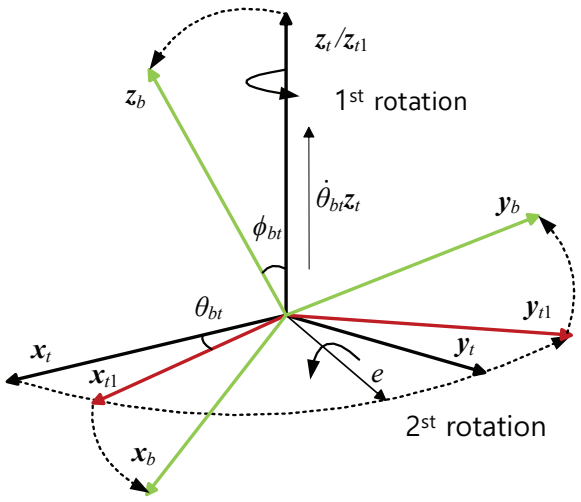

Fig. 1 Two rotations defining the orientation of frame $\mathcal{B}$ relative to frame $\mathcal{T}$

Then, we define the orientation of coordinate frame $\mathcal{B}$ with respect to $\mathcal{T}$ by two rotations. For the first rotation, frame $\mathcal{T}$ is rotated by an angle $\theta_{bt} \in [0,\ 2\pi)$ about $\boldsymbol{z}_t$ (positive counterclockwise), yielding an intermediate frame $\mathcal{T}_1$, whose basis vectors are denoted as $\{\boldsymbol{x}_{t1},\ \boldsymbol{y}_{t1},\ \boldsymbol{z}_{t1}\}$, as shown in Fig. 1. For the second rotation, frame $\mathcal{T}_1$ is rotated by an angle $\phi_{bt} \in [0,\ \pi)$ about the vector $\boldsymbol{e}$ (positive counterclockwise) to arrive at frame $\mathcal{B}$, as shown in Fig. 1.

The orientation of $\mathcal{B}$ with respect to $\mathcal{T}_1$ can be described by $\boldsymbol{z}_t \cdot \boldsymbol{z}_b$ and $\boldsymbol{z}_t \times \boldsymbol{z}_b$, where $\boldsymbol{z}_t \cdot \boldsymbol{z}_b = \cos\phi_{bt}$ represents the rotation angle, and $\boldsymbol{z}_t \times \boldsymbol{z}_b = \boldsymbol{e}\sin\phi_{bt}$ describes the rotation axis. The orientation of $\mathcal{T}'$ with respect to $\mathcal{T}$ can be described by the variable θ_{bt}. Thus, a new set of attitude parameters named σ-parameters, which describes the orientation of frame $\mathcal{B}$ with respect to frame $\mathcal{T}$, is defined as follows.

$$\boldsymbol{\sigma}_{bt} = \begin{bmatrix} \boldsymbol{z}_t \cdot \boldsymbol{z}_b \\ (\boldsymbol{z}_t \times \boldsymbol{z}_b) \cdot \boldsymbol{x}_b \\ (\boldsymbol{z}_t \times \boldsymbol{z}_b) \cdot \boldsymbol{y}_b \\ \theta_{bt} \end{bmatrix} = \begin{bmatrix} \cos\phi_{bt} \\ \boldsymbol{e} \cdot \boldsymbol{x}_b \sin\phi_{bt} \\ \boldsymbol{e} \cdot \boldsymbol{y}_b \sin\phi_{bt} \\ \theta_{bt} \end{bmatrix} \tag{1}$$

where $(\boldsymbol{z}_t \times \boldsymbol{z}_b) \cdot \boldsymbol{x}_b$ and $(\boldsymbol{z}_t \times \boldsymbol{z}_b) \cdot \boldsymbol{y}_b$ represent the first and the second components of $\boldsymbol{z}_t \times \boldsymbol{z}_b$ in frame $\mathcal{B}$ respectively. Since the third component of $\boldsymbol{z}_t \times \boldsymbol{z}_b$ in frame $\mathcal{B}$ is always zero, it is not given in the definition of $\boldsymbol{\sigma}_{bt}$. Let $\boldsymbol{\rho}_{bt}$ denote $[\boldsymbol{z}_t \cdot \boldsymbol{z}_b,\ (\boldsymbol{z}_t \times \boldsymbol{z}_b) \cdot \boldsymbol{x}_b,\ (\boldsymbol{z}_t \times \boldsymbol{z}_b) \cdot \boldsymbol{y}_b]^{\mathrm{T}}$. The new set of attitude parameters is then expressed as:

$$\boldsymbol{\sigma}_{bt} = \begin{bmatrix} \boldsymbol{\rho}_{bt} \\ \theta_{bt} \end{bmatrix} \tag{2}$$

where the constraint of $||\boldsymbol{\rho}_{bt}|| = 1$ is always satisfied.

B. Kinematics of the New Set of Attitude Parameters

1. *Kinematics of* $\boldsymbol{\rho}_{bt}$

Firstly, the kinematics of $\boldsymbol{\rho}_{bt}$ are derived as follows. The expression of $\boldsymbol{\rho}_{bt}$ can be simplified as

$$\boldsymbol{\rho}_{bt} = \begin{bmatrix} \boldsymbol{z}_t \cdot \boldsymbol{z}_b \\ \boldsymbol{z}_t \cdot \boldsymbol{y}_b \\ -\boldsymbol{z}_t \cdot \boldsymbol{x}_b \end{bmatrix} \tag{3}$$

where the identities $(\boldsymbol{a} \times \boldsymbol{b}) \cdot \boldsymbol{c} = -(\boldsymbol{c} \times \boldsymbol{b}) \cdot \boldsymbol{a}$, $\boldsymbol{x}_b \times \boldsymbol{z}_b = -\boldsymbol{y}_b$, and $\boldsymbol{y}_b \times \boldsymbol{z}_b = \boldsymbol{x}_b$ are used.

Taking the time derivative of $\boldsymbol{\rho}_{bt}$ gives

$$\dot{\boldsymbol{\rho}}_{bt} = \begin{bmatrix} -(\boldsymbol{\omega}_{bt} \times \boldsymbol{z}_t) \cdot \boldsymbol{z}_b \\ -(\boldsymbol{\omega}_{bt} \times \boldsymbol{z}_t) \cdot \boldsymbol{y}_b \\ (\boldsymbol{\omega}_{bt} \times \boldsymbol{z}_t) \cdot \boldsymbol{x}_b \end{bmatrix} = \begin{bmatrix} -(\boldsymbol{z}_t \times \boldsymbol{z}_b) \cdot \boldsymbol{\omega}_{bt} \\ -(\boldsymbol{z}_t \times \boldsymbol{y}_b) \cdot \boldsymbol{\omega}_{bt} \\ (\boldsymbol{z}_t \times \boldsymbol{x}_b) \cdot \boldsymbol{\omega}_{bt} \end{bmatrix} \tag{4}$$

where $\boldsymbol{\omega}_{bt}$ is the angular velocity of frame $\mathcal{B}$ relative to frame $\mathcal{T}$.

Decomposing the right hand side of Eq. (4) into frame $\mathcal{B}$ gives:

$$\dot{\boldsymbol{\rho}}_{bt} = \begin{bmatrix} -(\boldsymbol{z}_t \times \boldsymbol{z}_b) \cdot \boldsymbol{x}_b, & -(\boldsymbol{z}_t \times \boldsymbol{z}_b) \cdot \boldsymbol{y}_b, & -(\boldsymbol{z}_t \times \boldsymbol{z}_b) \cdot \boldsymbol{z}_b \\ -(\boldsymbol{z}_t \times \boldsymbol{y}_b) \cdot \boldsymbol{x}_b, & -(\boldsymbol{z}_t \times \boldsymbol{y}_b) \cdot \boldsymbol{y}_b, & -(\boldsymbol{z}_t \times \boldsymbol{y}_b) \cdot \boldsymbol{z}_b \\ (\boldsymbol{z}_t \times \boldsymbol{x}_b) \cdot \boldsymbol{x}_b, & (\boldsymbol{z}_t \times \boldsymbol{x}_b) \cdot \boldsymbol{y}_b, & (\boldsymbol{z}_t \times \boldsymbol{x}_b) \cdot \boldsymbol{z}_b \end{bmatrix} \boldsymbol{\omega}_{bt}^b \tag{5}$$

where $\boldsymbol{\omega}_{bt}^b$ is the body angular velocity relative to $\mathcal{T}$ frame, expressed in $\mathcal{B}$. With Eq. (1) and Eq. (3), Eq. (5) can be simplified as

$$\dot{\boldsymbol{\rho}}_{bt} = \begin{bmatrix} \dot{\rho}_0 \\ \dot{\rho}_1 \\ \dot{\rho}_2 \end{bmatrix} = \begin{bmatrix} -\rho_1 & -\rho_2 & 0 \\ \rho_0 & 0 & \rho_2 \\ 0 & \rho_0 & -\rho_1 \end{bmatrix} \boldsymbol{\omega}_{bt}^b \tag{6}$$

where ρ_0, ρ_1, and ρ_2 are the first, second and third element of $\boldsymbol{\rho}_{bt}$, respectively.

2. Kinematic of θ_{bt}

The kinematic of θ_{bt} is derived as follows. To express more concisely, let $\boldsymbol{a}^\times$ denote the cross product matrix of an arbitrary vector $\boldsymbol{a}$. From the properties of the direction cosine matrix, it follows that

$$\left(\boldsymbol{\omega}_{bt}^b\right)^\times = -\dot{\boldsymbol{C}}_{bt}\boldsymbol{C}_{bt}^{\mathrm{T}} \tag{7}$$

where $\boldsymbol{C}_{bt}$ is the direction cosine matrix from frame $\mathcal{T}$ to frame $\mathcal{B}$. $\boldsymbol{C}_{bt}$ can be derived from the definition of the two rotations shown in Fig. 1, and its expression is given by

$$\boldsymbol{C}_{bt} = \left(\cos\phi_{bt}\boldsymbol{I}_3 + (1-\cos\phi_{bt})\,\boldsymbol{e}^b\left(\boldsymbol{e}^b\right)^{\mathrm{T}} - \sin\phi_{bt}\left(\boldsymbol{e}^b\right)^\times\right)\boldsymbol{C}_z\left(\theta_{bt}\right) \tag{8}$$

where $\boldsymbol{e}^b$ is the components of $\boldsymbol{e}$ in frame $\mathcal{B}$, $\boldsymbol{I}_3$ denotes the identity matrix with 3 dimensions, and $\boldsymbol{C}_z\left(\theta_{bt}\right)$ is expressed as

$$\boldsymbol{C}_z\left(\theta_{bt}\right) = \begin{bmatrix} \cos\theta_{bt} & \sin\theta_{bt} & 0 \\ -\sin\theta_{bt} & \cos\theta_{bt} & 0 \\ 0 & 0 & 1 \end{bmatrix} \tag{9}$$

Substituting Eq. (8) into Eq. (7), and simplifying yields

$$\boldsymbol{\omega}_{bt}^b = \dot{\phi}_{bt}\boldsymbol{e}^b - \left(1-\cos\phi_{bt}\right)\left(\boldsymbol{e}^b\right)^\times \dot{\boldsymbol{e}}^b + \sin\phi_{bt}\dot{\boldsymbol{e}}^b + \dot{\theta}_{bt}\boldsymbol{z}_t^b \tag{10}$$

where the expression of $\dot{\boldsymbol{e}}^b$ can be easily derived by differentiating $\boldsymbol{e} = \dfrac{\boldsymbol{z}_t \times \boldsymbol{z}_b}{\sin\phi_{bt}}$ with respect to time in frame $\mathcal{B}$. The expression of $\dot{\boldsymbol{e}}^b$ is then given as follows.

$$\dot{\boldsymbol{e}}^b = \frac{\boldsymbol{\omega}_{bt}^b}{\tan\phi_{bt}} - \frac{\left(\left(\boldsymbol{z}_b^b\right)^{\mathrm{T}}\boldsymbol{\omega}_{bt}^b\right)\boldsymbol{z}_t^b}{\sin\phi_{bt}} - \frac{\boldsymbol{e}^b\dot{\phi}_{bt}}{\tan\phi_{bt}} \tag{11}$$

where $\boldsymbol{z}_t^b$ is the components of $\boldsymbol{z}_t$ in frame $\mathcal{B}$, and $\boldsymbol{z}_b^b$ is the components of $\boldsymbol{z}_b$ in frame $\mathcal{B}$.

To solve $\dot{\theta}_{bt}$ from Eq. (10), multiplying $\left(\boldsymbol{z}_t^b + \boldsymbol{z}_b^b\right)^{\mathrm{T}}$ at both left side of Eq. (10), substituting Eq. (11) into Eq. (10), and simplifying yields

$$\left(\boldsymbol{z}_t^b + \boldsymbol{z}_b^b\right)^{\mathrm{T}}\boldsymbol{\omega}_{bt}^b = \left(1+\cos\phi_{bt}\right)\dot{\theta}_{bt} - \frac{\left(1-\cos\phi_{bt}\right)}{\tan\phi_{bt}}\left(\boldsymbol{z}_t^b + \boldsymbol{z}_b^b\right)^{\mathrm{T}}\left(\boldsymbol{e}^b\right)^\times\boldsymbol{\omega}_{bt}^b + \cos\phi_{bt}\left(\boldsymbol{z}_t^b - \boldsymbol{z}_b^b\right)^{\mathrm{T}}\boldsymbol{\omega}_{bt}^b \tag{12}$$

where $\left(\boldsymbol{z}_t^b + \boldsymbol{z}_b^b\right)^{\mathrm{T}}\boldsymbol{e}^b = 0$, $\left(\boldsymbol{z}_t^b\right)^{\mathrm{T}}\boldsymbol{z}_b^b = \cos\phi_{bt}$, and $\left(\boldsymbol{z}_b^b\right)^{\mathrm{T}}\dot{\boldsymbol{e}}^b = 0$ are used. The last two items on the right hand side of Eq. (12) can be then eliminated when substituting $\boldsymbol{z}_b^b = [0,\ 0,\ 1]^{\mathrm{T}}$, $\boldsymbol{z}_t^b = [-\rho_2,\ \rho_1,\ \rho_0]^{\mathrm{T}}$, $\boldsymbol{e}^b\sin\phi_{bt} = [\rho_1,\ \rho_2,\ 0]^{\mathrm{T}}$, and $\rho_0 = \cos\phi_{bt}$ into Eq. (12). Thus, the kinematic of θ_{bt} is derived as

$$\dot{\theta}_{bt} = \left[-\frac{\rho_2}{1+\rho_0},\ \frac{\rho_1}{1+\rho_0},\ 1\right]\cdot\boldsymbol{\omega}_{bt}^b \tag{13}$$

3. Kinematics of $\boldsymbol{\sigma}_{bt}$

With the kinematics of $\boldsymbol{\rho}_{bt}$ and θ_{bt}, expressed in Eq. (6) and Eq. (13) respectively, the whole kinematics of σ-parameters are then given by

$$\dot{\boldsymbol{\sigma}}_{bt} = \begin{bmatrix} \dot{\rho}_0 \\ \dot{\rho}_1 \\ \dot{\rho}_2 \\ \dot{\theta}_{bt} \end{bmatrix} = \begin{bmatrix} -\rho_1 & -\rho_2 & 0 \\ \rho_0 & 0 & \rho_2 \\ 0 & \rho_0 & -\rho_1 \\ -\dfrac{\rho_2}{1+\rho_0} & \dfrac{\rho_1}{1+\rho_0} & 1 \end{bmatrix}\boldsymbol{\omega}_{bt}^b \tag{14}$$

C. Relations of σ-parameters and the corresponding direction cosine matrix

For a known $\boldsymbol{\sigma}_{bt}$, the direction cosine matrix from $\mathcal{T}$ to $\mathcal{B}$ can be calculated by

$$\boldsymbol{C}_{bt} = \left(\rho_0 \boldsymbol{I}_3 + \frac{\boldsymbol{\rho}_v \boldsymbol{\rho}_v{}^{\mathrm{T}}}{1+\rho_0} - \boldsymbol{\rho}_v{}^{\times}\right) \boldsymbol{C}_z\left(\theta_{bt}\right) \tag{15}$$

where $\boldsymbol{\rho}_v = [\rho_1,\ \rho_2,\ 0]^{\mathrm{T}}$.

For a known $\boldsymbol{C}_{bt}$, $\boldsymbol{\sigma}_{bt}$ can be calculated as follows. ρ_0 and $\boldsymbol{\rho}_v$ can be first calculated by

$$\rho_0 = \left(\boldsymbol{z}_t^b\right)^{\mathrm{T}} \boldsymbol{z}_b^b = \left(\boldsymbol{C}_{bt}\boldsymbol{z}_t^t\right)^{\mathrm{T}} \boldsymbol{z}_b^b \tag{16}$$

$$\boldsymbol{\rho}_v = \left(\boldsymbol{z}_t^b\right)^{\times} \boldsymbol{z}_b^b = \left(\boldsymbol{C}_{bt}\boldsymbol{z}_t^t\right)^{\times} \boldsymbol{z}_b^b \tag{17}$$

where $\boldsymbol{z}_t^t = \boldsymbol{z}_b^b = [0,\ 0,\ 1]^{\mathrm{T}}$. $\boldsymbol{C}_z\left(\theta_{bt}\right)$ can be then obtained by

$$\boldsymbol{C}_z\left(\theta_{bt}\right) = \left(\rho_0 \boldsymbol{I}_3 + \frac{\boldsymbol{\rho}_v \boldsymbol{\rho}_v{}^{\mathrm{T}}}{1+\rho_0} - \boldsymbol{\rho}_v{}^{\times}\right)^{\mathrm{T}} \boldsymbol{C}_{bt} \tag{18}$$

D. Properties of the New Set of Attitude Parameters

Based on the definition of σ-parameters in Eq. (3) and its kinematics in Eq. (14), the following properties are obtained.

If $\boldsymbol{\omega}_{bt}$ is chosen along the direction of $\boldsymbol{z}_t$, and expressed as $\boldsymbol{\omega}_{bt} = \omega_\theta \boldsymbol{z}_t$, ϕ_{bt} and $\boldsymbol{e}^b$ are both constant, but θ_{bt} changes with a rate of ω_θ. If $\boldsymbol{\omega}_{bt}$ is chosen along the direction of $\boldsymbol{e}$, and expressed as $\boldsymbol{\omega}_{bt} = \omega_\phi \boldsymbol{e}$, θ_{bt} and $\boldsymbol{e}^b$ are both constant, but ϕ_{bt} changes with a rate of ω_ϕ. Then, a approximate decoupled two rotations, $\boldsymbol{\omega}_{bt} = \omega_\theta \boldsymbol{z}_t$ and $\boldsymbol{\omega}_{bt} = \omega_\phi \boldsymbol{e}$, are obtained, which will be used to design the angular velocity trajectory of the spacecraft afterward.

III. Angular Velocity Trajectory Planning

This section firstly develops a new angular velocity trajectory based on the properties of σ-parameters. This new angular velocity trajectory is a space curve on a conic surface, which can be therefore used to avoid some unwanted points in angular velocity space. However, there is only one available angular velocity trajectory for a certain final attitude, since the rotation axes are limited as $\boldsymbol{z}_t$ and $\boldsymbol{e}$. To increase the number of the angular velocity trajectories, a more general type of angular velocity trajectory is developed based on a more general type of two rotations, whose

rotation axes are not limited to be $\boldsymbol{z}_t$ and $\boldsymbol{e}$. Consequently, the possibility of avoiding unwanted points is increased.

A. Angular Velocity Trajectory Based on the Properties of σ-parameters

To avoid some unwanted points in angular velocity space, a new angular velocity trajectory is developed based on the properties of σ-parameters. Different from the traditional trajectory (eigen-axis maneuver), the new angular velocity trajectory is a space curve instead of the curve on a certain axis (eigen-axis).

To design the new type of angular velocity trajectory, a reference frame $\mathcal{R}$ is first defined as follows. The origin is located at the center of mass of the spacecraft, and $\{\boldsymbol{x}_r, \boldsymbol{y}_r, \boldsymbol{z}_r\}$ are mutually orthogonal unit vectors satisfying the following constraints. At the begin of the maneuver, $\{\boldsymbol{x}_r, \boldsymbol{y}_r, \boldsymbol{z}_r\}$ are aligned with $\{\boldsymbol{x}_b, \boldsymbol{y}_b, \boldsymbol{z}_b\}$, and at the end of maneuver, $\{\boldsymbol{x}_r, \boldsymbol{y}_r, \boldsymbol{z}_r\}$ are aligned with $\{\boldsymbol{x}_t, \boldsymbol{y}_t, \boldsymbol{z}_t\}$. The orientation of frame $\mathcal{R}$ relative to frame $\mathcal{T}$ then describes the reference angular trajectory, which will be designed afterward. Before the development of the new angular velocity trajectory, some notations are defined as follows. Let $\boldsymbol{\sigma}_{rt}$ denote the orientation of frame $\mathcal{R}$ relative to frame $\mathcal{T}$. Let θ_{rt} denote the fourth element of $\boldsymbol{\sigma}_{rt}$, representing the first rotation angle from frame $\mathcal{T}$ to frame $\mathcal{R}$. Let ϕ_{rt} denote the angle between $\boldsymbol{z}_r$ and $\boldsymbol{z}_t$, which describes the second rotation angle from frame $\mathcal{T}$ to frame $\mathcal{R}$.

With these definitions, the objective of trajectory planning is summarized as designing a suitable angular velocity trajectory ensuring θ_{rt} and ϕ_{rt} arrive at zero as fast as possible. Based on the properties of σ-parameters, the angular velocity of frame $\mathcal{R}$ relative to frame $\mathcal{T}$ is designed as

$$\boldsymbol{\omega}_{rt} = \omega_\theta \boldsymbol{z}_t + \omega_\phi \boldsymbol{e} \tag{19}$$

where $\boldsymbol{e} = \dfrac{\boldsymbol{z}_t \times \boldsymbol{z}_r}{|\boldsymbol{z}_t \times \boldsymbol{z}_r|}$, and $\boldsymbol{\omega}_{rt}$ is the angular velocity of frame $\mathcal{R}$ relative to frame $\mathcal{T}$. To realize the angular velocity of Eq. (19), the following reference angular acceleration is needed.

$$\boldsymbol{a}_{rt} = \frac{d_I \boldsymbol{\omega}_{rt}}{dt} = \frac{d_r \boldsymbol{\omega}_{rt}}{dt} + \boldsymbol{\omega}_{rI} \times \boldsymbol{\omega}_{rt} \tag{20}$$

where $\dfrac{d_I()}{dt}$ and $\dfrac{d_r()}{dt}$ are the time derivative relative to frame $\mathcal{I}$ and frame $\mathcal{R}$, and $\boldsymbol{\omega}_{rI}$ is the angular velocity of frame $\mathcal{R}$ relative to frame $\mathcal{I}$.

Since the base vectors of frame $\mathcal{T}$ are fixed in inertial space, the relation $\boldsymbol{\omega}_{rI} = \boldsymbol{\omega}_{rt}$ holds. Substituting Eq. (19) into Eq. (20) gives

$$\boldsymbol{a}_{rt} = \omega_\theta \omega_\phi (\boldsymbol{z}_t \times \boldsymbol{e}) + \dot{\omega}_\theta \boldsymbol{z}_t + \dot{\omega}_\Phi \boldsymbol{e} \tag{21}$$

where $\dfrac{d_r \boldsymbol{z}_t}{dt} = -\boldsymbol{\omega}_{rt} \times \boldsymbol{z}_t$ and $\dfrac{d_r \boldsymbol{e}}{dt} = 0$ are used.

With the angular velocity of Eq. (19), the following relations are satisfied.

$$\dot{\theta}_{rt} = \omega_\theta \tag{22}$$

$$\dot{\phi}_{rt} = \omega_\phi \tag{23}$$

Thus, the reference angular trajectory can be designed by choosing suitable ω_θ and ω_ϕ to ensure θ_{rt} and ϕ_{rt} arrive at zero as fast as possible. The bang-off-bang maneuver, shown in Fig. 2, is used

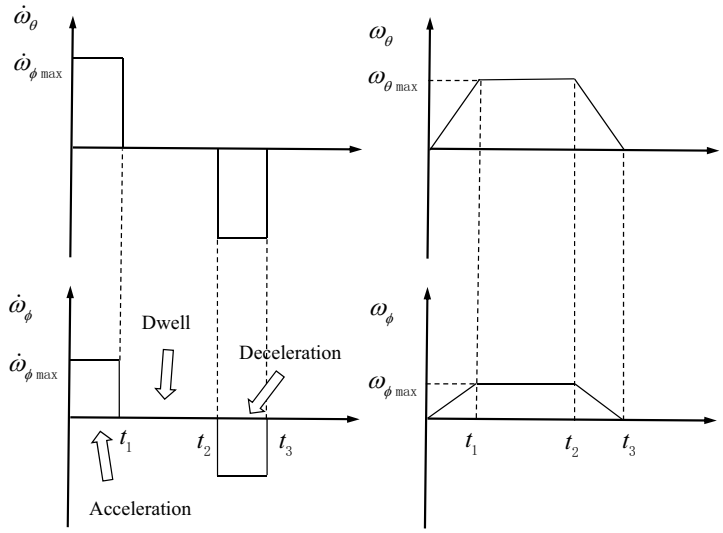

Fig. 2 Bang-off-bang type maneuver

as a reference trajectory when the constraints of angular velocity and angular acceleration are taken into account. To obtain a concise and explicit trajectory, the following constraints are considered.

$$\frac{\omega_{\theta\,\max}}{\omega_{\phi\,\max}} = \frac{\dot{\omega}_{\theta\,\max}}{\dot{\omega}_{\phi\,\max}} = \frac{|\theta_{rt0}|}{|\phi_{rt0}|} \tag{24}$$

where $\omega_{\phi\,\max}$, $\omega_{\theta\,\max}$, $\dot{\omega}_{\phi\,\max}$, and $\dot{\omega}_{\theta\,\max}$ are the maximum value of ω_ϕ, ω_θ, $\dot{\omega}_\phi$, and $\dot{\omega}_\theta$, respectively, and θ_{rt0} and ϕ_{rt0} are the initial value of θ_{rt} and ϕ_{rt}, respectively. With the constraint of Eq. (24),

the duration of acceleration region, dwell region, and deceleration region of θ_{rt} is the same as that of ϕ_{rt}, respectively. They can be calculated by the following equations.

$$t_1 = \frac{\omega_{\phi\,\max}}{\dot{\omega}_{\phi\,\max}} = \frac{\omega_{\theta\,\max}}{\dot{\omega}_{\theta\,\max}} \tag{25}$$

$$t_2 = \frac{|\phi_{rt0}|}{\omega_{\phi\,\max}} = \frac{|\theta_{rt0}|}{\omega_{\theta\,\max}} \tag{26}$$

$$t_3 = t_1 + t_2 \tag{27}$$

The expressions of $\dot{\omega}_\theta$ and $\dot{\omega}_\phi$ are given by

$$\dot{\omega}_\theta = \begin{cases} -\text{sign}\,(\theta_{rt0}) \cdot \dot{\omega}_{\theta\,\max}, & 0 < t \leq t_1 \\ 0, & t_1 < t \leq t_2 \\ \text{sign}\,(\theta_{rt0}) \cdot \dot{\omega}_{\theta\,\max}, & t_2 < t \leq t_3 \end{cases} \tag{28}$$

$$\dot{\omega}_\phi = \begin{cases} -\text{sign}\,(\phi_{rt0}) \cdot \dot{\omega}_{\phi\,\max}, & 0 < t \leq t_1 \\ 0, & t_1 < t \leq t_2 \\ \text{sign}\,(\phi_{rt0}) \cdot \dot{\omega}_{\phi\,\max}, & t_2 < t \leq t_3 \end{cases} \tag{29}$$

The expressions of ω_θ and ω_ϕ can be then obtained by integrating Eq. (28) and Eq. (29), and θ_{rt} and ϕ_{rt} can be then obtained by twice integrating Eq. (28) and Eq. (29).

Combined with Eq. (24), $\omega_{\phi\,\max}$, $\omega_{\theta\,\max}$, $\dot{\omega}_{\phi\,\max}$, and $\dot{\omega}_{\theta\,\max}$ are calculated by the following equations.

$$\omega_{\theta\,\max}^2 + \omega_{\phi\,\max}^2 = \omega_{\max}^2 \tag{30}$$

$$\dot{\omega}_{\theta\,\max}^2 + \dot{\omega}_{\phi\,\max}^2 + \omega_{\theta\,\max}^2 \omega_{\phi\,\max}^2 = a_{\max}^2 \tag{31}$$

where $a_{\max}$ is the maximum angular acceleration, and $\omega_{\max}$ is the maximum angular velocity.

The total angular velocity trajectory can be then divided into two parts. The first part is along the direction of $\boldsymbol{e}$ with the magnitude of ω_ϕ, the other part is along the direction of $\boldsymbol{z}_t$ with the magnitude of ω_θ. From the angular velocity in Eq. (19), it is observed that the direction of $\boldsymbol{e}$ is unchanged, but $\boldsymbol{z}_t$ rotates around $\boldsymbol{e}$ with a change rate $-\omega_\phi$. Therefore, the total angular velocity

trajectory is a space curve on a conic surface as shown in Fig. 3. The cone axis is $\boldsymbol{e}$ and the cone angle is $\arctan\dfrac{|\theta_{rt0}|}{|\phi_{rt0}|}$. This type of angular velocity trajectory is called cone-type angular velocity trajectory, which can be used to avoid some unwanted points in angular velocity space, such as impassable singular surface.

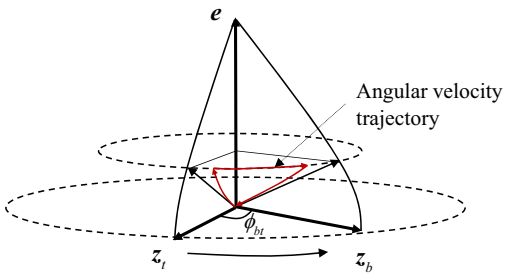

Fig. 3 Reference trajectory of angular velocity

B. Extended Angular Velocity Trajectory

1. General Type of Two Rotations

To increase the number of the cone-type angular velocity trajectory, a general type of two rotations whose rotation axes are not limited as $\boldsymbol{z}_t$ and $\boldsymbol{e}$ is developed. Before the development of this type of two rotations, some notations are defined as follows. Let $\boldsymbol{l}_b$ be a unit vector fixed in $\mathcal{B}$ frame, and let $\boldsymbol{l}_t$ be a unit vector fixed in $\mathcal{T}$ frame. The components of $\boldsymbol{l}_b$ in $\mathcal{B}$ frame are the same as those of $\boldsymbol{l}_t$ in $\mathcal{T}$ frame, i.e., $\boldsymbol{l}_b^b = \boldsymbol{l}_t^t$. Let $\boldsymbol{e}_b$ be a unit vector along the direction of $\boldsymbol{l}_t \times \boldsymbol{l}_b$, and let $\boldsymbol{e}_t$ be a unit vector which satisfies that the components of $\boldsymbol{e}_t$ in $\mathcal{T}$ frame are the same as those of $\boldsymbol{e}_b$ in $\mathcal{B}$ frame, i.e., $\boldsymbol{e}_b^b = \boldsymbol{e}_t^t$.

Then, a type of two rotations, which is performed on frame $\mathcal{T}$, are given as follows. For the first rotation shown in Fig. 4(a), frame $\mathcal{T}$ is rotated by an angle θ about $\boldsymbol{l}_t$ (positive counterclockwise) to align $\boldsymbol{e}_t$ with $\boldsymbol{e}_b$, yielding an intermediate frame. For the second rotation shown in Fig. 4(b), the intermediate frame is rotated by an angle ϕ about the vector $\boldsymbol{e}_b$ (positive counterclockwise) to align $\boldsymbol{l}_t$ with $\boldsymbol{l}_b$. After these two rotations, both $\boldsymbol{l}_t$ and $\boldsymbol{e}_t$ are aligned with $\boldsymbol{l}_b$ and $\boldsymbol{e}_b$ respectively, which implies frame $\mathcal{T}$ and frame $\mathcal{B}$ are aligned to each other. This type of two rotations is denoted by $Rot\{\boldsymbol{l}_t, \theta; \boldsymbol{e}_b, \phi\}$.

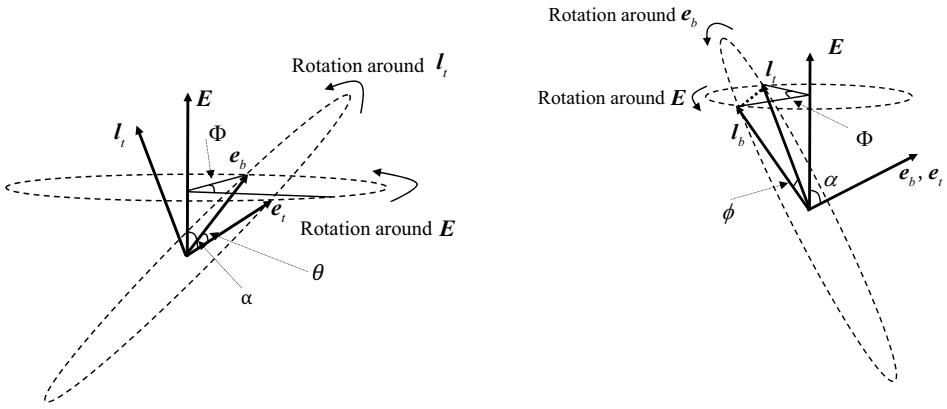

(a) (b)

Fig. 4 A general type of two rotations: a) first rotation about $\boldsymbol{l}_t$ b) second rotation about $\boldsymbol{e}_b$

To fully determine the parameters of $Rot\{\boldsymbol{l}_t, \theta; \boldsymbol{e}_b, \phi\}$, ϕ and θ should be derived first. Without loss of generality, the orientation of frame $\mathcal{B}$ relative to frame $\mathcal{T}$ is described by eigen-axis $\boldsymbol{E}$ and eigen-angle Φ, which means rotating frame $\mathcal{T}$ around $\boldsymbol{E}$ about Φ can align these two frames, where $\boldsymbol{E}$ and Φ can be obtained from the attitude determination system. The angle between $\boldsymbol{e}_b$ and $\boldsymbol{e}_t$, θ, can be then obtained by using the relations of spherical trigonometry shown in Fig. 4(a). Its expression is given by

$$\sin\frac{\theta}{2} = \sin\alpha \sin\frac{\Phi}{2} \tag{32}$$

where α is the angle between $\boldsymbol{E}$ and $\boldsymbol{e}_b$. In addition, The angle between $\boldsymbol{l}_b$ and $\boldsymbol{l}_t$, ϕ, is obtained using the relations of spherical trigonometry shown in Fig. 4(b). Its expression is given by

$$\tan\frac{\phi}{2} = \cos\alpha \tan\frac{\Phi}{2} \tag{33}$$

With the known variables of $\boldsymbol{E}$, Φ, and an arbitrarily given unit vector $\boldsymbol{e}_b$, all of the parameters of $Rot\{\boldsymbol{l}_t, \theta; \boldsymbol{e}_b, \phi\}$ can be obtained by the following steps.

First, α can be obtained by $\cos\alpha = \boldsymbol{e}_b \cdot \boldsymbol{E}$, and then θ and ϕ can be obtained by Eq. (32) and Eq. (33). Finally the first rotation axis $\boldsymbol{l}_t$ can be obtained by

$$\boldsymbol{l}_t \sin\alpha = \boldsymbol{e}_b \times (\boldsymbol{E} \times \boldsymbol{e}_b)\cos\frac{\phi}{2} + (\boldsymbol{E} \times \boldsymbol{e}_b)\sin\frac{\phi}{2} \tag{34}$$

where $\boldsymbol{l}_t$ can be chosen as arbitrary unit vector if $\sin\alpha = 0$.

Then, the orientation of frame $\mathcal{B}$ relative to frame $\mathcal{T}$, described by $\boldsymbol{E}$ and Φ, can also be described by a two rotations $Rot\{\boldsymbol{l}_t, \theta; \boldsymbol{e}_b, \phi\}$, where $\boldsymbol{e}_b$ can be arbitrarily chosen, and θ, ϕ, and $\boldsymbol{l}_t$ can be obtained from Eq. (32), Eq. (33) and Eq. (34), respectively.

2. Description of a General Type of Two Rotations with σ-Parameters

To develop an angular velocity trajectory similar with Eq. (19) for a general type of two rotations $Rot\{\boldsymbol{l}_t, \theta; \boldsymbol{e}_b, \phi\}$, $Rot\{\boldsymbol{l}_t, \theta; \boldsymbol{e}_b, \phi\}$ should be described by σ-parameters. To achieve this, two new coordinate frames, denoted by $\mathcal{B}'$ and $\mathcal{T}'$, are defined as follows. The origins of these two frames are both located at the center of mass of the spacecraft. The basis vectors of $\mathcal{B}'$, denoted by $\{\boldsymbol{x}_{b'}, \boldsymbol{y}_{b'}, \boldsymbol{z}_{b'}\}$, is defined as $\{\dfrac{\boldsymbol{l}_b \times \boldsymbol{z}_b}{\|\boldsymbol{l}_b \times \boldsymbol{z}_b\|}, \dfrac{\boldsymbol{l}_b \times (\boldsymbol{l}_b \times \boldsymbol{z}_b)}{\|\boldsymbol{l}_b \times \boldsymbol{z}_b\|}, \boldsymbol{l}_b\}$ which is fixed in frame $\mathcal{B}$, and the basis vectors of $\mathcal{T}'$, denoted by $\{\boldsymbol{x}_{t'}, \boldsymbol{y}_{t'}, \boldsymbol{z}_{t'}\}$, is defined as $\{\dfrac{\boldsymbol{l}_t \times \boldsymbol{z}_t}{\|\boldsymbol{l}_t \times \boldsymbol{z}_t\|}, \dfrac{\boldsymbol{l}_t \times (\boldsymbol{l}_t \times \boldsymbol{z}_t)}{\|\boldsymbol{l}_t \times \boldsymbol{z}_t\|}, \boldsymbol{l}_t\}$ which is fixed in frame $\mathcal{T}$.

The definitions of $\mathcal{B}'$ and $\mathcal{T}'$ ensure the following two conditions hold. The first condition is the cosine direction matrix from $\mathcal{B}'$ to $\mathcal{B}$ and that from $\mathcal{T}'$ to $\mathcal{T}$ are both equal to a constant matrix denoted by $\boldsymbol{C}$, expressed as

$$\boldsymbol{C} = \left[\frac{\boldsymbol{l}_t^t \times \boldsymbol{z}_t^t}{\|\boldsymbol{l}_t^t \times \boldsymbol{z}_t^t\|}, \frac{\boldsymbol{l}_t^t \times (\boldsymbol{l}_t^t \times \boldsymbol{z}_t^t)}{\|\boldsymbol{l}_t^t \times \boldsymbol{z}_t^t\|}, \boldsymbol{l}_t^t\right] = \left[\frac{\boldsymbol{l}_b^b \times \boldsymbol{z}_b^b}{\|\boldsymbol{l}_b^b \times \boldsymbol{z}_b^b\|}, \frac{\boldsymbol{l}_b^b \times (\boldsymbol{l}_b^b \times \boldsymbol{z}_b^b)}{\|\boldsymbol{l}_b^b \times \boldsymbol{z}_b^b\|}, \boldsymbol{l}_b^b\right] \tag{35}$$

where the relations of $\boldsymbol{l}_b^b = \boldsymbol{l}_t^t$ and $\boldsymbol{z}_b^b = \boldsymbol{z}_t^t = [0,\ 0,\ 1]^{\mathrm{T}}$ are used. The second condition is that the $\boldsymbol{z}$-axis of frame $\mathcal{B}'$ and frame $\mathcal{T}'$ are $\boldsymbol{l}_b$ and $\boldsymbol{l}_t$, respectively.

The first condition guarantees that frame $\mathcal{T}'$ and frame $\mathcal{B}'$ are aligned to each other if the two rotations of $Rot\{\boldsymbol{l}_t, \theta; \boldsymbol{e}_b, \phi\}$ are performed on frame $\mathcal{T}'$. Thus, the problem of controlling frame $\mathcal{B}$ to coincide with frame $\mathcal{T}$ can be converted to the problem of controlling frame $\mathcal{B}'$ to coincide with frame $\mathcal{T}'$.

The second condition guarantees that the two rotations of $Rot\{\boldsymbol{l}_t, \theta; \boldsymbol{e}_b, \phi\}$ from frame $\mathcal{T}'$ to frame $\mathcal{B}'$ can be described by the σ-parameters. The expression of σ-parameters is given by

$$\boldsymbol{\sigma}_{b't'} = \begin{bmatrix} \boldsymbol{z}_{t'} \cdot \boldsymbol{z}_{b'} \\ (\boldsymbol{z}_{t'} \times \boldsymbol{z}_{b'}) \cdot \boldsymbol{x}_{b'} \\ (\boldsymbol{z}_{t'} \times \boldsymbol{z}_{b'}) \cdot \boldsymbol{y}_{b'} \\ \theta_{b't'} \end{bmatrix} = \begin{bmatrix} \cos\phi_{b't'} \\ \boldsymbol{e}_b \cdot \boldsymbol{x}'_b \sin\phi_{b't'} \\ \boldsymbol{e}_b \cdot \boldsymbol{y}'_b \sin\phi_{b't'} \\ \theta_{b't'} \end{bmatrix} \tag{36}$$

where $\boldsymbol{\sigma}_{b't'}$ is the σ-parameters of frame $\mathcal{B}'$ with respect to frame $\mathcal{T}'$, and $\phi_{b't'}$ and $\theta_{b't'}$ are equal to ϕ and θ respectively, which can be obtained by Eq. (32) and Eq. (33). Thus, an angular velocity trajectory of frame $\mathcal{B}'$ relative to frame $\mathcal{T}'$ can be designed based on the method presented in Section III A.

3. Reference Trajectory for a General Type of Two Rotations

To design the reference trajectory of frame $\mathcal{B}'$ relative to frame $\mathcal{T}'$ using the method presented in Section III A, a reference frame $\mathcal{R}'$ is firstly defined as follows. The origin is located at the center of mass of the spacecraft, and $\{\boldsymbol{x}_{r'}, \boldsymbol{y}_{r'}, \boldsymbol{z}_{r'}\}$ are mutually orthogonal unit vectors, which satisfy the following constraints. At the begin of the maneuver, $\{\boldsymbol{x}_{r'}, \boldsymbol{y}_{r'}, \boldsymbol{z}_{r'}\}$ are aligned with $\{\boldsymbol{x}_{b'}, \boldsymbol{y}_{b'}, \boldsymbol{z}_{b'}\}$, and at the end of maneuver, $\{\boldsymbol{x}_{r'}, \boldsymbol{y}_{r'}, \boldsymbol{z}_{r'}\}$ are aligned with $\{\boldsymbol{x}_{t'}, \boldsymbol{y}_{t'}, \boldsymbol{z}_{t'}\}$. Let $\boldsymbol{\sigma}_{r't'}$ denote the relative attitude of frame $\mathcal{R}'$ relative to frame $\mathcal{T}'$. Let $\theta_{r't'}$ denote the fourth element of $\boldsymbol{\sigma}_{r't'}$, representing the first rotation angle from frame $\mathcal{R}'$ to frame $\mathcal{B}'$. Let $\phi_{r't'}$ denote the angle between $\boldsymbol{z}_{r'}$ and $\boldsymbol{z}_{b'}$, which represents the second rotation angle from frame $\mathcal{R}'$ to frame $\mathcal{B}'$.

Similar with Eq. (19), the reference angular velocity of frame $\mathcal{R}'$ relative to frame $\mathcal{T}'$, denoted by $\boldsymbol{\omega}_{r't'}$, is given as

$$\boldsymbol{\omega}_{r't'} = \omega_\theta \boldsymbol{l}_t + \omega_\phi \boldsymbol{e}_b \tag{37}$$

where $\boldsymbol{l}_t$ represents the $\boldsymbol{z}$-axis of frame $\mathcal{T}'$, and $\boldsymbol{e}_b$ denotes the unit vector along the direction of $\boldsymbol{z}'_t \times \boldsymbol{z}'_b$. Then, the following relations are satisfied.

$$\dot{\theta}_{r't'} = \omega_\theta \tag{38}$$

$$\dot{\phi}_{r't'} = \omega_\phi \tag{39}$$

Analogy with Eq. (22) and Eq. (23), ω_θ and ω_ϕ are designed as bang-off-bang type maneuver. ω_θ and ω_ϕ can be obtained by integrating Eq. (28) and Eq. (29), where θ_{rt0} and ϕ_{rt0} should be replaced by θ_0 and ϕ_0 respectively. θ_0 and ϕ_0 are the initial value of θ and ϕ respectively.

To realize the angular velocity of Eq. (37), the following reference angular acceleration is needed.

$$\boldsymbol{a}_{r't'} = \omega_\theta \omega_\phi (\boldsymbol{l}_t \times \boldsymbol{e}_b) + \dot{\omega}_\theta \boldsymbol{l}_t + \dot{\omega}_\phi \boldsymbol{e}_b \tag{40}$$

where $\dot{\omega}_\theta$ and $\dot{\omega}_\phi$ can be obtained by Eq. (28) and Eq. (29). θ_{rt0} and ϕ_{rt0} in Eq. (28) and Eq. (29) should be replaced by θ_0 and ϕ_0, respectively.

With the reference angular velocity trajectory of Eq. (37), the total angular velocity trajectory is then on a conic surface with a cone axis $\boldsymbol{e}_b$. Since $\boldsymbol{e}_b$ can be chosen as any unit vector, the number of feasible angular velocity trajectories is increased greatly.

IV. Attitude Tracking Controller

This section firstly introduces the dynamics and the kinematics of a rigid body spacecraft, and then develops an attitude tacking controller based on σ-parameters. Finally, the calculation procedure of commanded torque is presented.

A. Attitude Dynamics and Kinematics

To design the attitude controller, the dynamics of a rigid body spacecraft are then given by

$$\boldsymbol{J}\frac{d_{b'}\boldsymbol{\omega}_{b'r'}}{dt} + \boldsymbol{J}\frac{d_{b'}\boldsymbol{\omega}_{r'I}}{dt} + \boldsymbol{\omega}_{b'I} \times (\boldsymbol{J}\boldsymbol{\omega}_{b'I} + \boldsymbol{h}) = \boldsymbol{T} \tag{41}$$

where $\boldsymbol{J}$ is moment of inertia dyadic, $\dfrac{d_{b'}\,()}{dt}$ is the time derivative with respect to frame $\mathcal{B}'$, $\boldsymbol{\omega}_{b'r'}$ is the angular velocity of frame $\mathcal{B}'$ relative to frame $\mathcal{R}'$, $\boldsymbol{\omega}_{r'I}$ is the angular velocity of frame $\mathcal{R}'$ relative to frame $\mathcal{I}$, $\boldsymbol{h}$ is the total angular momentum vector of SGCMGs, and $\boldsymbol{T}$ is the command torque vector. In Eq. (41), $\dfrac{d_{b'}\boldsymbol{\omega}_{r'I}}{dt}$ can be written as

$$\frac{d_{b'}\boldsymbol{\omega}_{r'I}}{dt} = \frac{d_I\boldsymbol{\omega}_{r'I}}{dt} - \boldsymbol{\omega}_{b'I} \times \boldsymbol{\omega}_{r'I} = \frac{d_I\boldsymbol{\omega}_{r't'}}{dt} - \boldsymbol{\omega}_{b'r'} \times \boldsymbol{\omega}_{r't'} \tag{42}$$

where $\boldsymbol{\omega}_{r't'}$ is the angular velocity of frame $\mathcal{T}'$ relative to frame $\mathcal{R}'$, and $\boldsymbol{\omega}_{t'I} = 0$ is used. Substituting Eq. (42) into Eq. (41), and decomposing Eq. (41) into frame $\mathcal{B}'$ gives

$$\boldsymbol{J}^{b'}\dot{\boldsymbol{\omega}}^{b'}_{b'r'} + \boldsymbol{J}^{b'}\boldsymbol{a}^{b'}_{r't'} - \boldsymbol{J}^{b'}\left(\boldsymbol{\omega}^{b'}_{b'r'} \times \boldsymbol{\omega}^{b'}_{r't'}\right) + \boldsymbol{\omega}^{b'}_{b'I} \times \left(\boldsymbol{J}^{b'}\boldsymbol{\omega}^{b'}_{b'I} + \boldsymbol{h}^{b'}\right) = \boldsymbol{T}^{b'} \tag{43}$$

where the superscript b' represents the components of a vector or dyadic in frame $\mathcal{B}'$.

The orientation of frame $\mathcal{B}'$ relative to frame $\mathcal{R}'$ is described by σ-parameters, and the kinematics

are given by

$$\dot{\boldsymbol{\sigma}}_{b'r'} = \begin{bmatrix} \dot{\rho}_{0'} \\ \dot{\rho}_{1'} \\ \dot{\rho}_{2'} \\ \dot{\theta}_{b'r'} \end{bmatrix} = \begin{bmatrix} -\rho_{1'} & -\rho_{2'} & 0 \\ \rho_{0'} & 0 & \rho_{2'} \\ 0 & \rho_{0'} & -\rho_{1'} \\ -\dfrac{\rho_{2'}}{1+\rho_{0'}} & \dfrac{\rho_{1'}}{1+\rho_{0'}} & 1 \end{bmatrix} \boldsymbol{\omega}_{b'r'}^{b'} \tag{44}$$

where $\dot{\rho}_{0'} = \boldsymbol{z}_{r'} \cdot \boldsymbol{z}_{b'}$, $\dot{\rho}_{1'} = (\boldsymbol{z}_{r'} \times \boldsymbol{z}_{b'}) \cdot \boldsymbol{x}_{b'}$, and $\dot{\rho}_{2'} = (\boldsymbol{z}_{r'} \times \boldsymbol{z}_{b'}) \cdot \boldsymbol{y}_{b'}$.

B. Controller Design and Stability Analysis

The attitude tracking controller in frame $\mathcal{B}'$ is proposed as follows

$$\begin{aligned} \boldsymbol{T}^{b'} = \boldsymbol{J}^{b'} \left(-k_p \boldsymbol{\rho}_{v'} - k_p \theta_{b'r'} \boldsymbol{v}^{b'} - k_d \boldsymbol{\omega}_{b'r'}^{b'} + \boldsymbol{a}_{r't'}^{b'} \right) \\ + \boldsymbol{\omega}_{b'I}^{b'} \times \left(\boldsymbol{J}^{b'} \boldsymbol{\omega}_{b'I}^{b'} + \boldsymbol{h}^{b'} \right) - \boldsymbol{J}^{b'} \left(\boldsymbol{\omega}_{b'r'}^{b'} \times \boldsymbol{\omega}_{r't'}^{b'} \right) \end{aligned} \tag{45}$$

where the superscript b represents the components of a vector or dyadic in frame $\mathcal{B}$, k_p and k_d are positive control gains, $\boldsymbol{\rho}_{v'} = [\dot{\rho}_{1'},\ \dot{\rho}_{2'},\ 0]^{\mathrm{T}}$, and $\boldsymbol{v}^{b'} = \left[-\dfrac{\rho_{2'}}{1+\rho_{0'}},\ \dfrac{\rho_{1'}}{1+\rho_{0'}},\ 1 \right]^{\mathrm{T}}$.

Substituting the controller of Eq. (45) into the dynamic equations of Eq. (43), and simplifying gives

$$\dot{\boldsymbol{\omega}}_{b'r'}^{b'} = -k_p \boldsymbol{\rho}_{v'} - k_p \theta_{b'r'} \boldsymbol{v}^{b'} - k_d \boldsymbol{\omega}_{b'r'}^{b'} \tag{46}$$

To prove the stability of the resulting closed-loop system, the following candidate Lyapunov function V is proposed:

$$V = \frac{k_p}{2} \left(\boldsymbol{\rho}_{v'}^{\mathrm{T}} \boldsymbol{\rho}_{v'} + (1-\rho_{0'})^2 + \theta_{b'r'}^2 \right) + \frac{1}{2} \left(\boldsymbol{\omega}_{b'r'}^{b'} \right)^{\mathrm{T}} \boldsymbol{\omega}_{b'r'}^{b'} \tag{47}$$

For stability, the time derivative of V must be negative. Taking the time derivative of Eq. (47) results in

$$\dot{V} = k_p \boldsymbol{\rho}_{v'}^{\mathrm{T}} \dot{\boldsymbol{\rho}}_{v'} + k_p \rho_{0'} \dot{\rho}_{0'} - k_p \dot{\rho}_{0'} + k_p \theta_{b'r'} \dot{\theta}_{b'r'} + \left(\boldsymbol{\omega}_{b'r'}^{b'} \right)^{\mathrm{T}} \dot{\boldsymbol{\omega}}_{b'r'}^{b'} \tag{48}$$

Substituting Eq. (46) and into Eq. (48), and simplifying gives

$$\dot{V} = -k_p \left(\boldsymbol{\omega}_{b'r'}^{b'} \right)^{\mathrm{T}} \boldsymbol{\omega}_{b'r'}^{b'} \leq 0 \tag{49}$$

where $\dot{V}$ is a negative semidefinite function. Through Lyapunov's direct method, it can be shown that the equilibrium point $\boldsymbol{\rho}_{v'} = 0$, $\rho_{0'} = 1$, $\theta_{b'r'} = 0$ and $\boldsymbol{\omega}_{b'r'}^{b'} = 0$ is stable.

C. Calculation of the Commanded Torque

Since the actuators are installed in frame $\mathcal{B}$, the commanded torque in Eq. (45) should be given in frame $\mathcal{B}$ as follows.

$$\begin{aligned}\boldsymbol{T}^b = \boldsymbol{C}\boldsymbol{T}^{b'} = \boldsymbol{J}^b\left(-k_p\boldsymbol{C}\boldsymbol{\rho}_{v'} - k_p\theta_{b'r'}\boldsymbol{C}\boldsymbol{v}^{b'} - k_d\boldsymbol{\omega}^b_{b'r'} + \boldsymbol{a}^b_{r't'}\right)\\ +\boldsymbol{\omega}^b_{b'I}\times\left(\boldsymbol{J}^b\boldsymbol{\omega}^b_{b'I} + \boldsymbol{h}^b\right) - \boldsymbol{J}^b\left(\boldsymbol{\omega}^b_{b'r'}\times\boldsymbol{\omega}^b_{r't'}\right)\end{aligned} \tag{50}$$

where $\boldsymbol{C}$ can be obtained from Eq. (35), and $\boldsymbol{\rho}_{v'}$, $\boldsymbol{v}^{b'}$, $\boldsymbol{\omega}^b_{b'r'}$, $\boldsymbol{\omega}^b_{b'I}$, $\boldsymbol{\omega}^b_{r't'}$, and $\boldsymbol{a}^b_{r't'}$ can be obtained as follows.

1. *Calculation of $\boldsymbol{\rho}_{v'}$ and $\boldsymbol{v}^{b'}$*

$\boldsymbol{\omega}_{r't'}$ is designed as in Eq. (37), where ω_θ and ω_ϕ are obtained by integrating Eq. (28) and Eq. (29), where θ_{rt0} and ϕ_{rt0} should be replaced by θ_0 and ϕ_0, respectively. Thus, $\theta_{r't'}$ and $\phi_{r't'}$ can be obtained by integrating Eq. (38) and Eq. (39). They are expressed as

$$\theta_{r't'} = \int_0^t \omega_\theta dt \tag{51}$$

$$\phi_{r't'} = \int_0^t \omega_\phi dt \tag{52}$$

With $\theta_{r't'}$ and $\phi_{r't'}$, the orientation of frame $\mathcal{R}'$ relative to frame $\mathcal{T}'$ are obtained by

$$\boldsymbol{\sigma}_{r't'} = \begin{bmatrix}\cos\phi_{r't'}\\ \boldsymbol{e}_b\cdot\boldsymbol{x}_{r'}\sin\phi_{r't'}\\ \boldsymbol{e}_b\cdot\boldsymbol{y}_{r'}\sin\phi_{r't'}\\ \theta_{r't'}\end{bmatrix} \tag{53}$$

where $\boldsymbol{e}_b\cdot\boldsymbol{x}_{r'}$ and $\boldsymbol{e}_b\cdot\boldsymbol{y}_{r'}$ are the first and the second component of $\boldsymbol{e}_b$ in frame $\mathcal{R}'$, respectively. It is known that the components of $\boldsymbol{e}_b$ in frame $\mathcal{R}'$ are constant if $\boldsymbol{\omega}_{r't'}$ is given by Eq. (37). Thus, $\boldsymbol{e}_b\cdot\boldsymbol{x}_{r'}$ and $\boldsymbol{e}_b\cdot\boldsymbol{y}_{r'}$ can be obtained by

$$\boldsymbol{e}_b^{r'} = \begin{bmatrix}\boldsymbol{e}_b\cdot\boldsymbol{x}_{r'}\\ \boldsymbol{e}_b\cdot\boldsymbol{y}_{r'}\\ \boldsymbol{e}_b\cdot\boldsymbol{z}_{r'}\end{bmatrix} = \begin{bmatrix}\boldsymbol{e}_b\cdot\boldsymbol{x}_{r'0}\\ \boldsymbol{e}_b\cdot\boldsymbol{y}_{r'0}\\ \boldsymbol{e}_b\cdot\boldsymbol{z}_{r'0}\end{bmatrix} = \begin{bmatrix}\boldsymbol{e}_b\cdot\boldsymbol{x}_{b'0}\\ \boldsymbol{e}_b\cdot\boldsymbol{y}_{b'0}\\ \boldsymbol{e}_b\cdot\boldsymbol{z}_{b'0}\end{bmatrix} = \boldsymbol{C}^{\mathrm{T}}\boldsymbol{e}_b^{b0} \tag{54}$$

where the subscript, 0, represents the initial value of corresponding variable, $\boldsymbol{e}_b^{b0}$ is to be designed, which represents the components of the second rotation axis $\boldsymbol{e}_b$ in the initial frame of $\mathcal{B}$, $\boldsymbol{e}_b^{r'}$ represents

the components of $\boldsymbol{e}_b$ in frame $\mathcal{R}'$, and $\boldsymbol{C}$ is a constant matrix which can be obtained from Eq. (35). The fact that frame $\mathcal{R}'$ and frame $\mathcal{B}'$ are initially aligned is used to derive Eq. (54).

With $\boldsymbol{\sigma}_{r't'}$, the direction cosine matrix $\boldsymbol{C}_{r't'}$ from $\mathcal{T}'$ to $\mathcal{R}'$, can be obtained according to the property of σ-parameters in Eq. (15). $\boldsymbol{C}_{b'r'}$ can be then obtained by

$$\boldsymbol{C}_{b'r'} = \boldsymbol{C}_{b't'}\boldsymbol{C}_{r't'}^{\mathrm{T}} \tag{55}$$

where $\boldsymbol{C}_{b't'}$ is obtained by

$$\boldsymbol{C}_{b't'} = \boldsymbol{C}^{\mathrm{T}}\boldsymbol{C}_{bt}\boldsymbol{C} \tag{56}$$

where $\boldsymbol{C}_{bt}$ is obtained from the attitude determination system.

With $\boldsymbol{C}_{b'r'}$, the elements of $\boldsymbol{\sigma}_{b'r'}$ can be obtained in real time by the following equations.

$$\begin{bmatrix} \rho_{0'} \\ \boldsymbol{\rho}_{v'} \end{bmatrix} = \begin{bmatrix} \left(\boldsymbol{C}_{b'r'} \cdot \boldsymbol{z}_{r'}^{r'}\right)^{\mathrm{T}} \boldsymbol{z}_{r'}^{r'} \\ \left(\boldsymbol{C}_{b'r'} \cdot \boldsymbol{z}_{r'}^{r'}\right)^{\times} \boldsymbol{z}_{r'}^{r'} \end{bmatrix} \tag{57}$$

where $\boldsymbol{z}_{r'}^{r'} = [0,\ 0,\ 1]^{\mathrm{T}}$. $\theta_{b'r'}$ can be then obtained by

$$\boldsymbol{C}_z\left(\theta_{b'r'}\right) = \left(\rho_{0'}\boldsymbol{I}_3 + \frac{\boldsymbol{\rho}_{v'}{\boldsymbol{\rho}_{v'}}^{\mathrm{T}}}{1+\rho_{0'}} - {\boldsymbol{\rho}_{v'}}^{\times}\right)^{\mathrm{T}} \boldsymbol{C}_{b'r'} \tag{58}$$

With the obtained $\rho_{0'}$ and $\boldsymbol{\rho}_{v'}$, $\boldsymbol{v}^{b'} = \left[-\frac{\rho_{2'}}{1+\rho_{0'}},\ \frac{\rho_{1'}}{1+\rho_{0'}},\ 1\right]^{\mathrm{T}}$ can be then obtained.

2. Calculation of $\boldsymbol{\omega}_{r't'}^{b}$, $\boldsymbol{\omega}_{b'r'}^{b}$, and $\boldsymbol{\omega}_{b'I}^{b}$

$\boldsymbol{\omega}_{r't'}^{b}$ can be obtained by decomposing Eq. (37) into frame $\mathcal{B}$, expressed by

$$\boldsymbol{\omega}_{r't'}^{b} = \omega_\theta \boldsymbol{l}_t^b + \omega_\phi \boldsymbol{e}_b^b \tag{59}$$

where $\boldsymbol{e}_b^b$ can be calculated by

$$\boldsymbol{e}_b^b = \boldsymbol{C}_{br'}\boldsymbol{e}_b^{r'} = \boldsymbol{C}\boldsymbol{C}_{b'r'}\boldsymbol{C}^{\mathrm{T}}\boldsymbol{e}_b^{b0} \tag{60}$$

where $\boldsymbol{e}_b^{b0}$ is to be designed, which denotes the components of the second rotation axis $\boldsymbol{e}_b$ in the initial frame of $\mathcal{B}$, and $\boldsymbol{C}_{br'}$ represents the direction cosine matrix from frame $\mathcal{R}'$ to frame $\mathcal{B}$.

In Eq. (59), $\boldsymbol{l}_t^b$ can be obtained by

$$\boldsymbol{l}_t^b = \boldsymbol{C}\boldsymbol{C}_{b't'}\boldsymbol{l}_t^{t'} \tag{61}$$

where $\boldsymbol{l}_t^{t'} = \boldsymbol{z}_{t'}^{t'} = [0,\ 0,\ 1]^{\mathrm{T}}$. Thus, $\boldsymbol{\omega}_{b'r'}^b$ are obtained by

$$\boldsymbol{\omega}_{b'r'}^b = \boldsymbol{\omega}_{b't'}^b - \boldsymbol{\omega}_{r't'}^b \tag{62}$$

where $\boldsymbol{\omega}_{b't'}^b = \boldsymbol{\omega}_{bt}^b$ since the direction cosine matrix from frame $\mathcal{B}'$ to $\mathcal{B}$ and that from frame $\mathcal{T}'$ to $\mathcal{T}$ are both equal to the constant matrix $\boldsymbol{C}$, and $\boldsymbol{\omega}_{bt}^b$ can be obtained by the measurement of gyros.

Finally, $\boldsymbol{\omega}_{b'I}^b = \boldsymbol{\omega}_{bt}^b$ since the angular velocity of frame $\mathcal{B}'$ relative to $\mathcal{B}$, and the angular velocity of frame $\mathcal{T}$ relative to $\mathcal{I}$ are both zero.

3. Calculation of $\boldsymbol{a}_{r't'}^b$

$\boldsymbol{a}_{r't'}^b$ can be obtained as follows by decomposing Eq. (40) into frame $\mathcal{B}$

$$\boldsymbol{a}_{r't'}^b = \omega_\theta \omega_\phi (\boldsymbol{l}_t^b \times \boldsymbol{e}_b^b) + \dot{\omega}_\theta \boldsymbol{l}_t^b + \dot{\omega}_\Phi \boldsymbol{e}_b^b \tag{63}$$

V. Selection of Rotation Axes to Avoid the Impassable Singular States

This section firstl introduces the classification and determination of the singular states of S-GCMG, and then proposes a method to select the suitable second rotation axis in the initial frame of $\mathcal{B}$, denoted by $\boldsymbol{e}_b^{b0}$. As a result, the impassable singular states can be avoided. The selection of rotation aixs is based on the inverse dymamics method, which was introduced in [25, 26].

A. Torque-Produced Equation and Singularity

For a n-SGCMG system, the torque-produced equation is given by

$$\boldsymbol{T} = -h_0 \boldsymbol{A} \dot{\boldsymbol{\delta}} \tag{64}$$

where h_0 is the angular momentum magnitude of each SGCMG, $\boldsymbol{\delta}$ is a n-column vector whose i^{th} element represents the gimbal angle of the i^{th} SGCMG, $\dot{\boldsymbol{\delta}}$ is a n-column vector whose ith element represents the gimbal rate of the i^{th} SGCMG, and $\boldsymbol{A}$ is the Jacobian matrix, which is given by

$$\boldsymbol{A} = [\boldsymbol{t}_1,\ \boldsymbol{t}_2, \cdots,\ \boldsymbol{t}_n] \tag{65}$$

where $\boldsymbol{t}_i$ is the torque unit vector of the ith SGCMG.

The rank of $\boldsymbol{A}$ is reduced to 2 at some specific gimbal angle combinations where the SGCMG system can not generate torque in a certain direction perpendicular to $\boldsymbol{t}_i$. This is called a singular

direction, and the unit vector in the singular direction is denoted by $\boldsymbol{u}$. These gimbal angle combinations are called singular states, and the corresponding states in angular momentum space is called singular surface, which can be obtained by

$$\boldsymbol{H}_s = \sum_{i=1}^{n} \varepsilon_i \frac{(\boldsymbol{g}_i \times \boldsymbol{u}) \times \boldsymbol{g}_i}{|\boldsymbol{g}_i \times \boldsymbol{u}|} \quad \text{where} \;\; \boldsymbol{u} \neq \pm \boldsymbol{g}_i \tag{66}$$

where $\boldsymbol{g}_i$ is the i^{th} gimbal axis vector, and $\varepsilon_i = \text{sign}\,(\boldsymbol{h}_i \cdot \boldsymbol{u}) = \pm 1$, where $\boldsymbol{h}_i$ is the angular momentum unit vector of the i^{th} SGCMG. The singular surface can then be directly obtained by considering all possible combinations of ε_i and all possible orientation of $\boldsymbol{u}$ on the unit sphere except $\boldsymbol{u} = \pm \boldsymbol{g}_i$. The singular surface is classified as passable singular surface and impassable singular surface based on the changes of angular momentum in the direction of $\boldsymbol{u}$ at a singular state [4], which can be expressed as

$$\boldsymbol{u} \cdot d\boldsymbol{H}_s = -\frac{h_0}{2} \boldsymbol{b}^{\mathrm{T}} \boldsymbol{Q}^S \boldsymbol{b} - \frac{h_0}{2} \boldsymbol{c}^{\mathrm{T}} \boldsymbol{Q}^N \boldsymbol{c} \tag{67}$$

where $\boldsymbol{b}$ is an arbitrary 2-column vector, $\boldsymbol{c}$ an arbitrary $(n-2)$-column vector,

$$\boldsymbol{Q}^S = \left[\boldsymbol{e}_1^S \;\; \boldsymbol{e}_2^S\right]^{\mathrm{T}} \boldsymbol{P}^{-1} \left[\boldsymbol{e}_1^S \;\; \boldsymbol{e}_2^S\right] \tag{68}$$

$$\boldsymbol{Q}^N = \left[\boldsymbol{e}_1^N \;\; \boldsymbol{e}_2^N \;\; \cdots \;\; \boldsymbol{e}_{n-2}^N\right]^{\mathrm{T}} \boldsymbol{P}^{-1} \left[\boldsymbol{e}_1^N \;\; \boldsymbol{e}_2^N \;\; \cdots \;\; \boldsymbol{e}_{n-2}^N\right] \tag{69}$$

where $\boldsymbol{P}$ is a diagonal matrix whose i^{th} diagonal element is $\dfrac{1}{\boldsymbol{u} \cdot \boldsymbol{h}_i}$, $\boldsymbol{e}_i^S$ is the i^{th} base of singularly constrained tangent space, and $\boldsymbol{e}_i^N$ is the i^{th} base of null motion space.

The term of $-\dfrac{h_0}{2} \boldsymbol{b}^{\mathrm{T}} \boldsymbol{Q}^S \boldsymbol{b}$ in Eq. (67) describes the motion on a singular surface, and therefore $-\dfrac{h_0}{2} \boldsymbol{b}^{\mathrm{T}} \boldsymbol{Q}^N \boldsymbol{b}$ determines the passability of the singular surface. If $\boldsymbol{Q}^N$ is indefinite, the angular momentum can pass the singular surface from one side to the other side, then the corresponding singular surface is passable. If $\boldsymbol{Q}^N$ is definite, then any gimbal rates can only make the angular momentum move on one side of the singular surface, i.e., the singular surface is impassable.

B. Singularity in Gimbal Angle Space

At a singular point in angular momentum space, the corresponding gimbal angles are several sets of continuous manifolds in gimbal angles space [4]. However, only one set of the manifolds contains a singular state. Therefore, the impassable singular surface is not really impassable, which

depend on whether the corresponding solution in gimbal angle space is singular state or not. An example is given in Fig. 5 to illustrate this phenomenon. In Fig. 5, the angular momentum $\boldsymbol{H}$ moves from $\boldsymbol{H}_1$ to $\boldsymbol{H}_3$, and an impassable singular surface is encountered when $\boldsymbol{H}$ equals $\boldsymbol{H}_2$. At this point, the corresponding solution in domain A is not a singular state, but the corresponding solution in domain B is a singular state. Therefore, if the initial gimbal angles belong to domain A, no singular state will be encountered when passing this impassable singular surface, but if the initial gimbal angles belong to domain B, the impassable singular state is sure to be encountered when $\boldsymbol{H}$ equals $\boldsymbol{H}_2$. This example indicates that an impassable singular surface is passable if the initial gimbal angles is selected correctly.

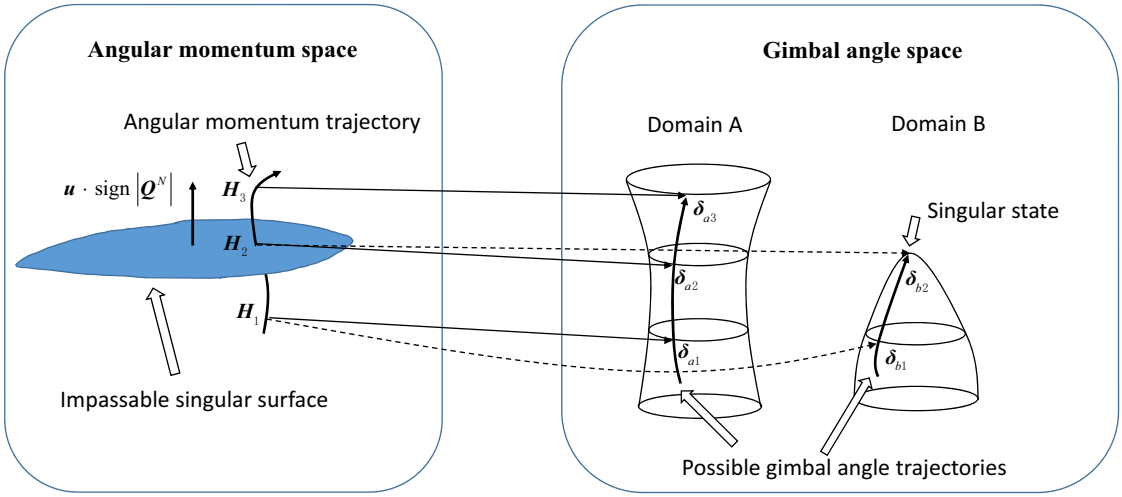

Fig. 5 Relation between singular surface and the corresponding solutions in gimbal angle space

With the analysis mentioned above, the standing problem is to find the condition that guarantees no singular state is encountered when passing an impassable singular surface. Since $\boldsymbol{Q}^N$ is definite at an impassable singular surface, the following inequality always holds at an impassable singular surface.

$$\boldsymbol{u}_{new}\cdot d\boldsymbol{H}_s \le 0 \tag{70}$$

where

$$\boldsymbol{u}_{new} = \mathrm{sign}\left|\boldsymbol{Q}^N\right|\cdot\boldsymbol{u} \tag{71}$$

where $\mathrm{sign}\left|\boldsymbol{Q}^N\right|\cdot\boldsymbol{u}$ denotes the sign of the determinant of $\boldsymbol{Q}^N$, and $\mathrm{sign}\left|\boldsymbol{Q}^N\right|\cdot\boldsymbol{u}$ denotes the singular

vector since $\text{sign}\left|\boldsymbol{Q}^N\right| \cdot \boldsymbol{u}$ equals either $\boldsymbol{u}$ or $-\boldsymbol{u}$.

Eq. (70) indicates that the angular momentum can only move in one side of the impassable singular surface in $-\boldsymbol{u}_{new}$ when an impassable singular state is nearly approached, which implies that the corresponding gimbal angle of an angular momentum in the other side in the direction of $\boldsymbol{u}_{new}$ must belong to the domain without a singular state. This situation is illustrated by an example in Fig. 5, where the solutions in the gimbal space, corresponding to the angular momentum $\boldsymbol{H}_3$ in the side of singular surface in the direction of $\boldsymbol{u}_{new}$, are sure to be in the Domain A where the singular state does not exist. However, the corresponding gimbal angle of $\boldsymbol{H}_1$ in the side in the direction of $-\boldsymbol{u}_{new}$ can belong to one of Domain A and Domain B. Therefore, if the angular momentum moves from $\boldsymbol{H}_3$ to $\boldsymbol{H}_1$, no singular state will be encountered. However, if the angular momentum moves from $\boldsymbol{H}_1$ to $\boldsymbol{H}_3$, the singular state may be encountered.

Thus, the following conclusion is obtained. If the angular momentum trajectory passes through an impassable singular surface from the side in the direction of $\boldsymbol{u}_{new}$ to the other side in the direction of $-\boldsymbol{u}_{new}$, no singular state will be encountered. This situation can be described by

$$\boldsymbol{u}_{new} \cdot \boldsymbol{T}_r \leq 0 \tag{72}$$

where $\boldsymbol{T}_r$ represents the change rate of the reference angular momentum.

This conclusion is significant to determine whether an impassable singular state in gimbal angle space will be encountered or not, when a angular momentum trajectory passes an impassable singular surface.

C. Selection of Suitable Angular Momentum Trajectory

To pass through an impassable singular surface using the cone-type of angular velocity trajectory, the following three steps are presented to select the suitable second rotation axis in the initial frame of $\mathcal{B}$, denoted by $\boldsymbol{e}_b^{b0}$, to avoid the impassable singular state with minimum maneuver time.

1) Calculate all points on the impassable singular surface, and then store these points and the corresponding singular vectors. The details of this step are given as follows.

First, for a certain singular vector $\boldsymbol{u}$, calculate the corresponding Jacobian matrix $\boldsymbol{A}_s$ by using

the following equation.

$$\boldsymbol{A}_s = [\boldsymbol{t}_{s1},\ \boldsymbol{t}_{s2},\ \cdots,\ \boldsymbol{t}_{sn}] \tag{73}$$

where $\boldsymbol{t}_{si}$ is expressed as

$$\boldsymbol{t}_{si} = \varepsilon_i \frac{(\boldsymbol{g}_i \times \boldsymbol{u})}{|\boldsymbol{g}_i \times \boldsymbol{u}|} \quad \text{where} \quad \boldsymbol{u} \neq \pm \boldsymbol{g}_i \tag{74}$$

Second, decomposing $\boldsymbol{A}_s$ using the singular value decomposition method gives

$$\boldsymbol{A}_s = \begin{bmatrix} \boldsymbol{c}_1 & \boldsymbol{c}_2 & \boldsymbol{u} \end{bmatrix} \begin{bmatrix} \gamma_1^2 & 0 & 0 & \cdots & 0 \\ 0 & \gamma_2^2 & 0 & \cdots & 0 \\ 0 & 0 & 0 & \cdots & 0 \end{bmatrix} \begin{bmatrix} \boldsymbol{e}_1^C & \boldsymbol{e}_2^C & \boldsymbol{e}_1^N & \cdots & \boldsymbol{e}_{n-2}^N \end{bmatrix}^{\mathrm{T}} \tag{75}$$

where $\boldsymbol{c}_1$ and $\boldsymbol{c}_2$ are the orthogonal basis of torque-producing space, $\boldsymbol{e}_1^C$ and $\boldsymbol{e}_2^C$ are the orthogonal basis of the complementary subspace of null-space, and γ_1 and γ_2 are the singular values of $\boldsymbol{A}_s$.

Third, calculate $\boldsymbol{Q}^N$ using Eq. (69), and determine the definiteness of $\boldsymbol{Q}^N$. If $\boldsymbol{Q}^N$ is definite (corresponding to an impassable singular surface), store the corresponding $\boldsymbol{u}_{new}$ and $\boldsymbol{H}_s$, which are calculated by Eq. (66) and Eq. (71), respectively.

Finally, take $\boldsymbol{u}$ over a sphere except for $\boldsymbol{u} \neq \pm \boldsymbol{g}_i$, and repeat the previous steps. The j^{th} stored $\boldsymbol{u}_{new}$ and $\boldsymbol{H}_s$ are then denoted by $\boldsymbol{u}_{newj}$ and $\boldsymbol{H}_{sj}$, respectively.

2) For a certain $\boldsymbol{e}_b^{b0}$, determine the minimum distance between the corresponding angular momentum trajectory and the impassable singular surface. The details are given as follows.

First, calculate the reference angular momentum trajectory and the reference torque trajectory using the following equations.

$$\boldsymbol{H}_r = \boldsymbol{J}^b \boldsymbol{\omega}_{r'I}^b = \boldsymbol{J}^b \boldsymbol{\omega}_{r't'}^b \tag{76}$$

$$\boldsymbol{T}_r = \boldsymbol{J}^b \boldsymbol{a}_{r'I}^b = \boldsymbol{J}^b \boldsymbol{a}_{r't'}^b \tag{77}$$

where $\boldsymbol{H}_r$ is the reference angular momentum trajectory expressed in frame $\mathcal{B}$, and $\boldsymbol{T}_r$ is the reference torque trajectory expressed in frame $\mathcal{B}$. $\boldsymbol{\omega}_{r't'}^b$ and $\boldsymbol{a}_{r't'}^b$ can be calculated by Eq. (59) and Eq. (63) respectively, where $\dot{\omega}_\theta$ and $\dot{\omega}_\phi$ are obtained from Eq. (28) and Eq. (29) by replacing θ_{rt0} and ϕ_{rt0}

with θ_0 and ϕ_0 respectively. θ_0 and ϕ_0 can be obtained by Eq. (32) and Eq. (33). In addition, $\boldsymbol{C}_{b'r'}$ is set to be an identity matrix during the calculation of $\boldsymbol{H}_r$ and $\boldsymbol{T}_r$.

Second, discretize $\boldsymbol{H}_r$ and $\boldsymbol{T}_r$ as m points, and calculate the minimum distance from the k^{th} point to the impassable singular surface using the following equations.

$$D_k = \min_j \sqrt{\left(\boldsymbol{H}_{rk} - \boldsymbol{H}_{sj}\right)^{\mathrm{T}} \left(\boldsymbol{H}_{rk} - \boldsymbol{H}_{sj}\right)} \tag{78}$$

where $\boldsymbol{H}_{rk}$ is the k^{th} point of $\boldsymbol{H}_r$, and D_k is the minimum distance from $\boldsymbol{H}_{rk}$ to the impassable singular surface.

Third, for the k^{th} point on the reference angular momentum trajectory, check whether the following condition is satisfied or not.

$$\boldsymbol{u}_{newl} \cdot \boldsymbol{T}_{rk} \leq 0 \tag{79}$$

where $\boldsymbol{T}_{rk}$ is the k^{th} point of $\boldsymbol{T}_r$, and l represents the optimal solution of j in Eq. (78). If Eq. (79) holds, replace D_k with a large value since the condition of Eq. (79) indicates that no impassable singular state will be encountered even if D_k equals zero.

Finally, take the value of k from 1 to m, and then calculate the minimum value of D_k using the following equation.

$$M = \min_k D_k \tag{80}$$

where M represents the minimum distance between the reference angular momentum trajectory and the impassable singular surface.

3) Take $\boldsymbol{e}_b^{b0}$ over a sphere, and repeat 2) to calculate the corresponding M and the maneuver time t_3, and then find the minimum maneuver time and the corresponding $\boldsymbol{e}_b^{b0}$ under the following constraint.

$$M \geq M_{safe} \tag{81}$$

where M_{safe} is the safe distance between the reference angular momentum trajectory and the impassable singular surface.

Based on the previous three steps, the optimal $\boldsymbol{e}_b^{b0}$ can be obtained if it exists.

VI. Numerical Simulations

In this section, simulations are performed to verify the effectiveness of the proposed SGCMG singularity avoidance method. In the simulations, the first 4 units of a regular dodecahedron configuration are selected, which is shown in Fig. 6. β is chosen as $\beta = 64.3°$. Therefore, the unit angular momentum and unit torque of each SGCMG are given by

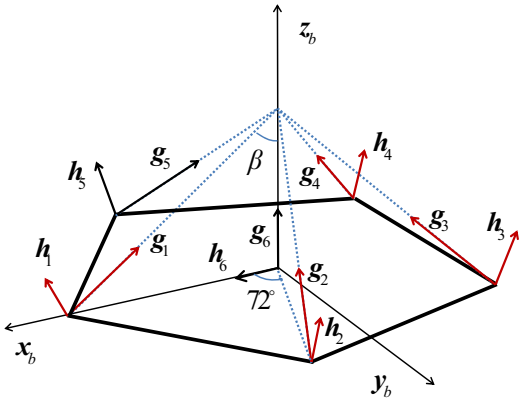

Fig. 6 SGCMG configuration

$$\boldsymbol{h}_i = \begin{bmatrix} \cos\left(i \times 72°\right)\cos\beta\cos\delta_i - \sin\left(i \times 72°\right)\sin\delta_i \\ \sin\left(i \times 72°\right)\cos\beta\cos\delta_i + \cos\left(i \times 72°\right)\sin\delta_i \\ \sin\beta\cos\delta_i \end{bmatrix}, \quad i = 1, 2, 3, 4 \tag{82}$$

$$\boldsymbol{t}_i = \begin{bmatrix} -\sin\left(i \times 72°\right)\cos\delta_i - \cos\left(i \times 72°\right)\cos\beta\sin\delta_i \\ \cos\left(i \times 72°\right)\cos\delta_i - \sin\left(i \times 72°\right)\cos\beta\sin\delta_i \\ -\sin\beta\sin\delta_i \end{bmatrix}, i = 1, 2, 3, 4 \tag{83}$$

Since the design of the reference trajectory guarantees that the impassable singular states in gimbal angle space will not be encountered, the steering law are chosen as the pseudo-inverse solution with null motions [1], which can avoid all passable singular states. This steering law is given as

$$\dot{\boldsymbol{\delta}} = -\frac{1}{h_0}\boldsymbol{A}^{\mathrm{T}}\left(\boldsymbol{A}\boldsymbol{A}^{\mathrm{T}}\right)^{-1}\boldsymbol{T} + k\left(\boldsymbol{I}_4 - \boldsymbol{A}^{\mathrm{T}}\left(\boldsymbol{A}\boldsymbol{A}^{\mathrm{T}}\right)^{-1}\boldsymbol{A}\right)\frac{\partial D}{\partial \boldsymbol{\delta}} \tag{84}$$

where D is the singular measurement, expressed as

$$D = \sum_{i \neq j}\left(\boldsymbol{t}_i \times \boldsymbol{t}_j\right)^{\mathrm{T}}\left(\boldsymbol{t}_i \times \boldsymbol{t}_j\right) \tag{85}$$

The simulation parameters are presented in Table. 1, where $\boldsymbol{\sigma}_{bt0}$ is the initial attitude of frame $\mathcal{B}$ relative to frame $\mathcal{T}$, $\boldsymbol{\omega}_{bt0}^{b}$ is the initial angular velocity of frame $\mathcal{B}$ relative to frame $\mathcal{T}$ in frame $\mathcal{B}$, and $\boldsymbol{\delta}_0$ is the initial gimbal angle. Then, the initial value of $\boldsymbol{E}$ in frame $\mathcal{B}$ and that of Φ, representing the initial orientation of frame $\mathcal{B}$ relative to frame $\mathcal{T}$, can be obtained as $[-0.8275,\ -0.5260,\ 0.1965]^{\mathrm{T}}$ and 2 rad, respectively. In addition, frame $\mathcal{B}$ is initially aligned with frame $\mathcal{I}$. With the parameters in Table. 1, the optimal $\boldsymbol{e}_b^{b0}$ is then obtained by the method developed in Section V. The optimal value of $\boldsymbol{e}_b^{b0}$ is given by

$$\boldsymbol{e}_b^{b0} = [-0.9419,\ 0.1110,\ 0.3171]^{\mathrm{T}} \tag{86}$$

With Eq. (32) and Eq. (33), θ_0 and ϕ_0 are then obtained as -1.1009 rad and 1.7683 rad respectively. With Eq. (24), Eq. (30) and Eq. (31), $\omega_{\theta\max}$, $\omega_{\phi\max}$, $a_{\theta\max}$ and $a_{\phi\max}$ are obtained as 0.0264 rad/s, 0.0424 rad/s, 0.0033 rad/s^2 and 0.0020 rad/s^2, respectively. Thus, with Eq. (25)-Eq. (27), t_1, t_2 and t_3 are obtained as 12.892 s, 41.660 s and 54.552 s, respectively.

Table 1 Simulation parameters

Parameter	Value
$\boldsymbol{I}^b$	$\begin{bmatrix} 2500 & -50 & -15 \\ -50 & 1800 & 32 \\ -15 & 32 & 2430 \end{bmatrix}$ kg $\cdot$ m^2
k_p	0.16
k_d	0.288
$\boldsymbol{\sigma}_{bt0}$	$[-0.3615,\ 0.6061,\ 0.7085,\ -0.5939]^{\mathrm{T}}$
$\boldsymbol{\omega}_{bt0}^{b}$	$[0,\ 0,\ 0]^{\mathrm{T}}$ rad/s
$\omega_{\max}$	0.05 rad/s
$a_{\max}$	0.005 rad/s^2
h_0	50 Nm $\cdot$ s
M_{safe}	5 Nm $\cdot$ s
k	0.05
$\boldsymbol{\delta}_0$	$[-2.2354,\ -1.3763,\ 0.0835,\ -2.1810]^{\mathrm{T}}$ rad

For comparison, two cases are considered in the simulations. In case 1, the reference trajectory of spacecraft angular velocity is generated according to the bang-off-bang eigen-axis maneuver. In case 2, the reference trajectory is generated by the proposed method.

A. Case 1

The simulation results for Case 1 are shown in Fig. 7 and Fig. 8. Fig. 8 shows the curve of singular measurement, where the singular measurement arrives at 0 at 6.7s, which indicates that an impassable singular surface is encountered. The required gimbal rates shown in Fig. 7(a) then becomes infinity.

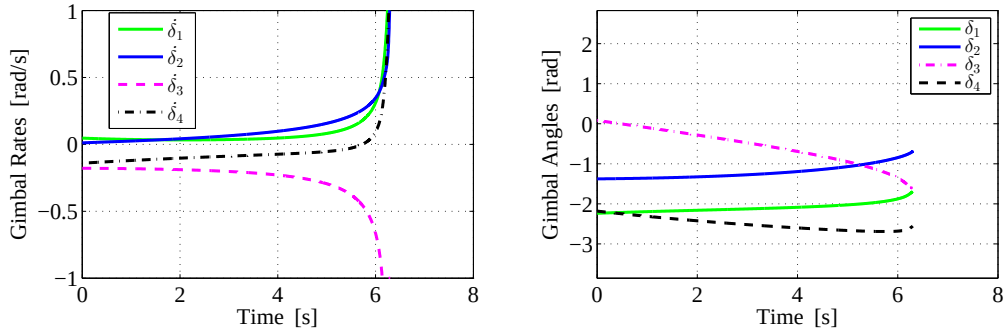

(a) (b)

Fig. 7 Gimbal rates and gimbal angles for Case 1: a) gimbal rates b) gimbal angles

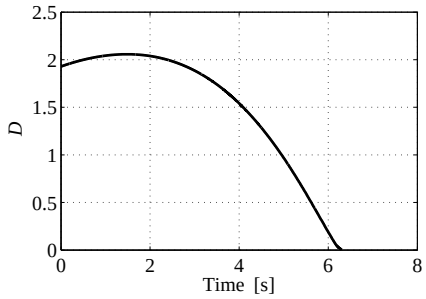

Fig. 8 Singular measurement for Case 1

B. Case 2

The simulation results for Case 2 are shown in Fig. 9-Fig. 12. Fig. 9 shows the gimbal rates and gimbal angles. Fig. 10 shows the curve of singular measurement, where the singular measurement is always greater than zero, which indicates that no impassable state is encountered during the maneuver. Fig. 11 shows the attitude information, where the σ-parameter of frame $\mathcal{B}$ relative to frame $\mathcal{T}$ is shown in Fig. 11(a), and angular velocity of frame $\mathcal{B}$ relative to frame $\mathcal{T}$ is shown in Fig. 11(b). Fig. 11(a) and Fig. 11(b) indicates that σ-parameter are valid, and the attitude controller

with σ-parameter can control the attitude converges to the target attitude. Fig. 12 shows the angular momentum trajectory, where the surface is the impassable singular surface. From Fig. 12, it is observed that the angular momentum trajectory has no intersection with the impassable surface during the acceleration region. However, the angular momentum trajectory intersects with the impassable singular surface in the deceleration region, but there is still no singular state occurred since the condition of Eq. (72) is satisfied at the intersection.

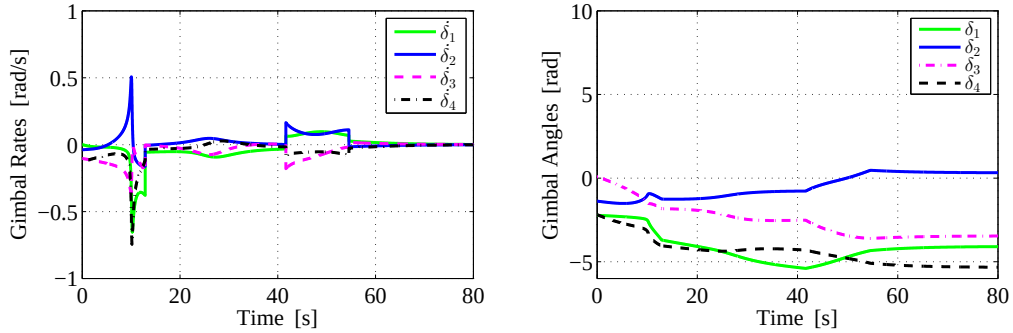

(a) (b)

Fig. 9 Gimbal rates and gimbal angles for Case 2: a) gimbal rates b) gimbal angles

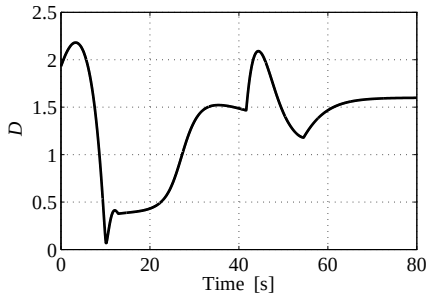

Fig. 10 Singular measurement for Case 2

VII. Conclusions

A SGCMG singularity avoidance method is developed by planning the angular momentum trajectory based on the proposed σ-parameter. The developed angular momentum trajectory of spacecraft is a cone-type of trajectory which is constructed from two approximate decoupling rotations. Then, suitable rotation axes are chosen to avoid impassable singular states during attitude maneuver of spacecraft. The advantages of this singularity avoidance method are summarized as

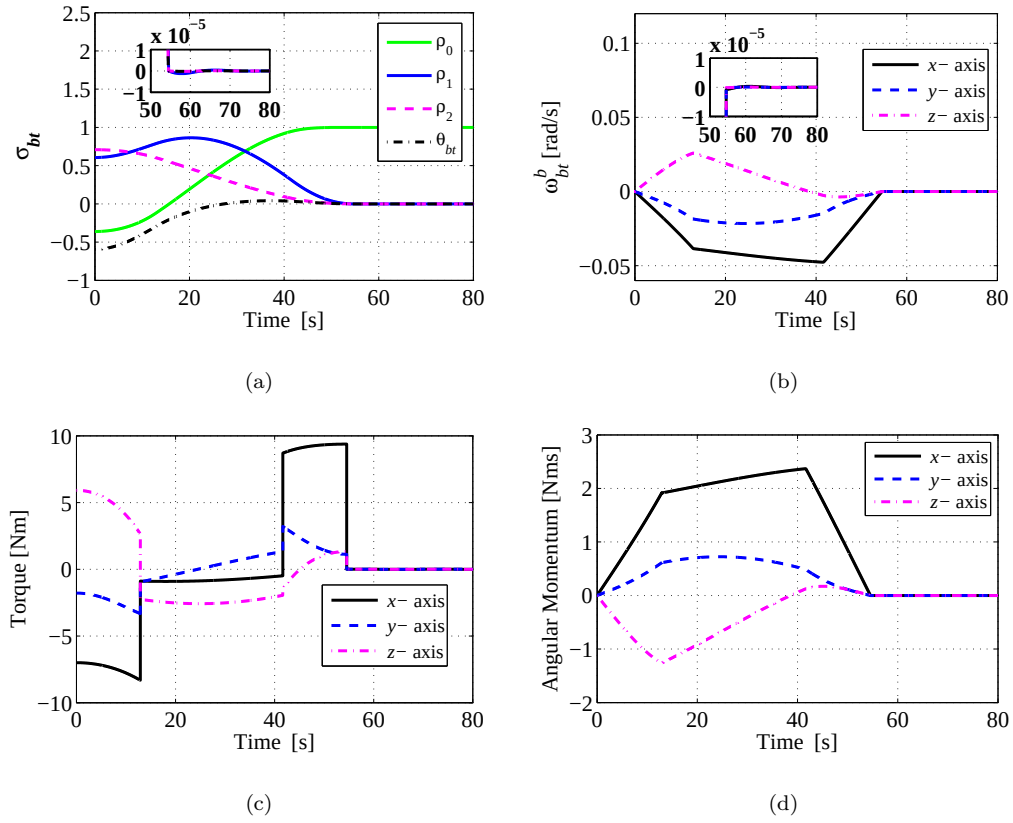

Fig. 11 Attitude information for Case 2: a) σ-parameter b) angular rates c) control torque d) angular momentum

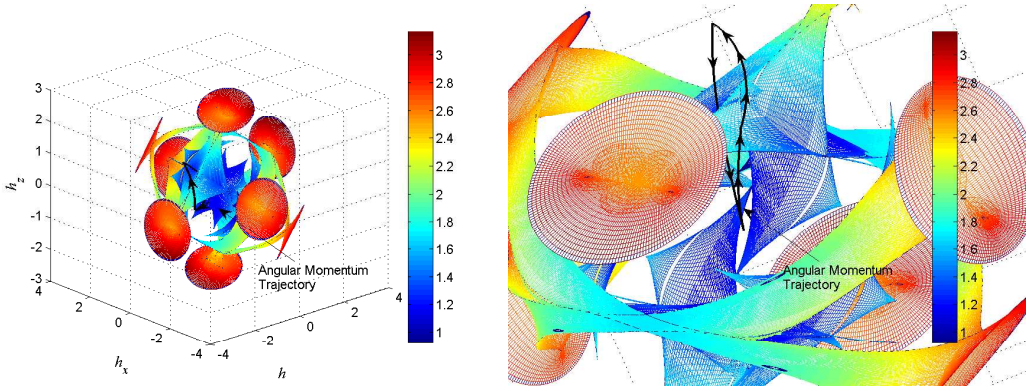

Fig. 12 Trajectory of angular momentum for Case 2: a) global graph b) part graph

follows. First, a simple steering law, which can only avoid the passable singular states, is only required for the SGCMG singularity avoidance because no impassable singular state is encountered with the proposed method. Second, some unavoidable impassable singular states in gimbal angles space can be avoided by using the proposed method.

Acknowledgements

Funded under the National Natural Science Foundation of China (61503093, 91438202, 61603115), Project Agreement No. AUGA5710053114 with Harbin Institute of Technology, and Open Fund of National Defense Key Discipline Laboratory of Micro-Spacecraft Technology (Grant Number HIT.KLOF.MST.201502).

References

[1] Bedrossian, N. S., Paradiso, J., Bergmann, E. V., "Steering Law Design for Redundant Single-Gimbal Control Moment Gyroscopes," *Journal of Guidance, Control, and Dynamics*, Vol. 13, No. 6, 1990, pp. 1083-1089.
doi:10.2514/3.20582

[2] Bedrossian, N. S., Paradiso, J., Bergmann, E. V., and Rowell, D., "Redundant Single Gimbal Control Moment Gyroscope Singularity Analysis," *Journal of Guidance, Control, and Dynamics*, Vol. 13, No. 6, 1990, pp. 1096-1101.
doi: 10.2514/3.20584

[3] Margulies, G., and Aubrun, J. N., "Geometric Theory of Single-Gimbal Control Moment Gyro System," *Journal of the Astronautical Sciences*, Vol. 26, No. 2, 1978, pp. 159-191.

[4] Kurokawa, H., "A Geometric Study of Single Gimbal Control Moment Gyros-Singularity and Steering Law," Ph.D. Dissertation, Aeronautics and Astronautics, Univ. Tokyo, Tokyo, 1997; Report of Mechanical Engineering Laboratory, No. 175, 1998.

[5] Kurokawa, H., "Survey of theory and steering laws of single-gimbal control moment gyros" *Journal of Guidance, Control, and Dynamics*, Vol. 30, No. 5, 2007, pp. 1331-1340.
doi: 10.2514/1.27316

[6] Vadali, S. R., Walker, S. R., Oh, H. S., "Preferred Gimbal Angles for Single Gimbal Control Moment Gyros," *Journal of Guidance, Control, and Dynamics*, Vol. 13, No. 6, 1990, pp. 1090-1095.
doi: 10.2514/3.20583

[7] Paradiso, J. A., "Global Steering of Single Gimballed Control Moment Gyroscopes Using A Directed Search," *Journal of Guidance, Control, and Dynamics*, Vol. 15, No. 5, 1992, pp. 1236-1244.
doi: 10.2514/3.20974

[8] Nakamura, Y., and Hanafusa, H., "Inverse Kinematic Solutions with Singularity Robustness for Robot Manipulator Control," *Journal of Dynamic Systems, Measurement, and Control*, Vol. 108, No. 3, 1986,

pp. 163-171.

doi:10.1115/1.3143764

[9] Ford, K. A., and Hall, C. D., "Singular Direction Avoidance Steering for Control Moment Gyros," *Journal of Guidance, Control, and Dynamics*, Vol. 23, No. 4, 2000, pp. 648-656.

doi: 10.2514/2.4610

[10] Jin, J., Zhang, J., Liu, Z., "Output-Torque Error Analysis and Steering Law Design of SGCMGs Based on SVD Theory". *AIAA Guidance, Navigation, and Control Conference*, AIAA 2009-5804, Chicago, Illinois, 2009, pp. 1-13.

doi: 10.2514/6.2009-5804

[11] Yamada, K. and Jikuya, I., "Directional Passability and Quadratic Steering Logic for Pyramid-type Single Gimbal Control Moment Gyros". *Acta Astronautica*, Vol. 102, 2014, pp. 103-123.

doi: org/10.1016/j.actaastro.2014.05.022

[12] Wie, B., Heiberg, C., and Bailey, D., "Singularity Robust Steering Logic for Redundant Single-Gimbal Control Moment Gyros," *Journal of Guidance, Control, and Dynamics*, Vol. 24, No. 5, 2001, pp. 865-872.

doi: 10.2514/2.4799

[13] Wie, B., "Singularity Analysis and Visualization for Single-Gimbal Control Moment Gyro Systems," *Journal of Guidance, Control, and Dynamics*, Vol. 27, No. 2, 2004, pp. 271-282.

doi: 10.2514/1.9167

[14] Wie, B., "Singularity Escape/Avoidance Steering Logic for Control Moment Gyro Systems," *Journal of Guidance, Control, and Dynamics*, Vol. 28, No. 5, 2005, pp. 948-956.

doi: 10.2514/1.10136

[15] Leve, F. A., and Fitz-Coy, N. G., "Hybrid Steering Logic for Single-Gimbal Control Moment Gyroscopes," *Journal of Guidance, Control, and Dynamics*, Vol. 33, No. 4, 2010, pp. 1202-1212.

doi: 10.2514/1.46853

[16] Takada, K., Kojima, H., and Matsuda, N., "Control Moment Gyro Singularity-Avoidance Steering Control Based on Singular-Surface Cost Function," *Journal of Guidance, Control, and Dynamics*, Vol. 33, No. 5, 2010, pp. 1442-1450.

doi: 10.2514/1.48381

[17] Kurokawa, H., "Exact Singularity Avoidance Control of The Pyrimid Type CMG system," *AIAA Guidance, Navigation, and Control Conference*, AIAA 94-3359-CP, Scottsdale, AZ, 1994, pp. 170-180.

doi: 10.2514/6.1994-3559

[18] Kurokawa, H., "Constrained Steering Law of Pyramid-Type Control Moment Gyros and Ground Tests," *Journal of Guidance, Control, and Dynamics*, Vol. 20, No. 3, 1997, pp. 445-449.
doi: 10.2514/2.4095

[19] Kanzawa, T., Haruki, M., and Yamanaka, K., "Steering Law of Control Moment Gyroscopes for Agile Attitude Maneuvers," *Journal of Guidance, Control, and Dynamics*, Vol. 39, No. 4, 2016, pp. 949-959.
doi: 10.2514/1.G001261

[20] Wu, C., Xu, R., Zhu, S., and Cui, P., "Time-optimal Spacecraft Attitude Maneuver Path Planning under Boundary and Pointing Constraints," *Acta Astronautica*, Vol. 137, 2017, pp. 128-137.
doi: org/10.1016/j.actaastro.2017.04.004

[21] Melton, R. G., "Hybrid Methods for Determining Time-optimal, Constrained Spacecraft Reorientation Maneuvers," *Acta Astronautica*, Vol. 94, No. 1, 2014, pp. 294-301.
doi: org/10.1016/j.actaastro.2013.05.007

[22] Turner, J. D., and Junkins, J. L., "Optimal Large-Angle Single-Axis Rotational Maneuvers of Flexible Spacecraft," *Journal of Guidance, Control, and Dynamics*, Vol. 3, No. 6, 1980, pp. 578-585.
doi: 10.2514/3.56036

[23] Singhose, W., Eloundou, R., and Lawrence, J., "Command Generation for Flexible Systems by Input Shaping and Command Smoothing," *Journal of Guidance, Control, and Dynamics*, Vol. 33, No. 6, 2010, pp. 1697-1707.
doi: 10.2514/1.50270

[24] Cole, M. O. T., and Wongratanaphisan, T., "Optimal FIR Input Shaper Designs for Motion Control With Zero Residual Vibration," *Journal of Guidance, Control, and Dynamics*, Vol. 133, No. 2, 2011: 021008.
doi: 10.1115/1.4003097

[25] Spiller, D., Ansalone, L., and Curti, F., "Particle Swarm Optimization for Time-Optimal Spacecraft Reorientation with Keep-Out Cones," Journal of Guidance, Control, and Dynamics, Vol.39, No.2, 2016, pp.312-325.
doi: 10.2514/1.G001228

[26] Basu, K. and Melton, R., "Time-optimal reorientation via inverse dynamics: A quaternion and particle swarm formulation," Advances in the Astronautical Sciences, Vol.156, 2016, pp.1631-1646, Astrodynamics Specialist Conference, August 2015.